UNIVERSITAT POLITÈCNICA DE VALÈNCIA

School of Telecommunications Engineering

Simulation of a MU-MIMO System in a Wi-Fi Environment

Master's Thesis

Master's Degree in Telecommunication Engineering

AUTHOR: Barreda Beltrán, Alberto

Tutor: Gómez Barquero, David

ACADEMIC YEAR: 2021/2022

Resumen:

En este trabajo se ha realizado un estudio de las técnicas multiusuario en sistemas de múltiple entrada y salida (MU-MIMO) en Wi-Fi, desde la primera versión pero centrándose en Wi-Fi 6 la versión más reciente que se centra en las técnicas de multiusuario. El estudio se centra en la simulación de estas técnicas en distintos escenarios utilizando Matlab. En el estudio se comparan los distintos precodificadores y decodificadores y se busca la configuración que obtiene la máxima capacidad. La comparación primero es centra en la comunicación con solo un usuario, variando principalmente el receptor, a continuación, el caso multiusuario variando principalmente el transmisor y finalmente se comparan entre ambos.

Resum:

En aquest treball s'ha realitzat un estudi de les tècniques multiusuari en sistemes de múltiple entrada i eixida (MU-MIMO) en Wi-Fi, des dels primer estàndards però centrant-nos en Wi-Fi 6 el més recent que es centra en les tècniques de multiusuari. L'estudi es centra en la simulació d'aquestes tècniques en diferents escenaris utilitzant Matlab. En les simulacions es comparen el precodificadors i els detectors i es busca la configuració que ofereix la màxima capacitat. La comparativa primerament es centra en la comunicació amb un sol usuari, variant principalment el receptor, a continuació el cas multiusuari variant principalment el transmissor i finalment es comparen entre ells.

Summary:

This project is based on a study of the techniques for multiuser multiple input multiple output (MU-MIMO) in Wi-Fi, starting on the initial releases but focussing on Wi-Fi 6 the most recent release which focuses on multiuser techniques. The study focusses on the simulation of this techniques in different scenarios using Matlab. In the simulations we compare the different precoders and detectors and look for the configuration that maximizes capacity.. The simulation firstly focuses on the single user communications where the receiver changes the most, then we simulate multiuser scenarios where the focus is on the transmitter; finally, we compare both.

INDEX

1. Introduction

Wi-Fi technology has become one of the most important technologies in our day to day lives, especially since the popularization of smartphones, tablets, laptops, and other connected devices at our homes. Its standard has and keeps evolving to keep up with the user's needs. Since the inception of the standard [1], it has adopted new techniques, from the orthogonal frequency division multiplexing (OFDM) as a modulation technique or the introduction of multiple antennas with the multiple input multiple output (MIMO) technologies. Since the Wi-Fi 6 version the focus of the standard included the ability to service multiple users at the same time with techniques like orthogonal frequency division multiple access (OFDMA) which allows the users to use the spectrum at the same time despite the full bandwidth usage on Wi-Fi. or, the focus of this thesis, multiuser MIMO which separates the users spatially creating parallel data streams and assigning them to different users.

Wi-Fi is the given name to the 802.11 technology from the institute of electrical and electronics engineering (IEEE). The IEEE 802 technical standards family covers the local area networks (LAN) specifying the physical layer (PHY) and medium access control (MAC). The main focus of the thesis is on the PHY layer which is the responsible of the capacity increases and coverture improvements. Since the original release in 1997 the standard has evolved through multiple versions with the most recent one being Wi-Fi 6 ratified in 2021.

1.1. Motivation

The MU-MIMO technique is one of the most promising enhancements for any wireless communication technique due to the improvements we can see on latency and capacity on any network with multiple devices. Despite being incorporated in the standard each implementation still needs to find the highest efficiency archivable for their application. These techniques are a recent addition to the Wi-Fi standard, initially incorporated as an optional feature on Wi-Fi 5, introduced as mandatory on the most recent release, Wi-Fi 6 as one of its core elements and will be expanded upon in the future Wi-Fi 7 version of the standard

This thesis is the result of the project developed during an internship at the company Maxlinear, that during the internship was finishing the development of the

version two of the Wi-Fi 6 chip and was starting the development of the Wi-Fi 7 version under the pre-releases of the standard.. This project served the purpose of researching and analysing in detail the standard, helping the team to obtain a more general view of it thanks to the multiple presentation realized during the internship, furthermore the simulations helped evaluating the MU-MIMO communications strengths and weaknesses.

2. Wi-Fi 6

2.1. Initial Wi-Fi standards

The first Wi-Fi standard [2] release in 1997, had a MAC standard resembling the recently successful Ethernet with a distributed access protocol, carrier sense multiple access (CSMA). This standard listens the medium determining if the channel is "idle" when the user checks it proceeds to transmit, in the other hand if its "busy" it will defer the transmission. In the wireless environment the collisions cannot be detected directly making them more costly than in the wired mediums. Instead of applying the collision detection from Ethernet it incorporates a collision avoidance where after waiting for the channel to be "idle" it waits a second random backoff time to avoid multiple stations to start the transmission at the same time.

The Wi-Fi technology utilizes the unlicenced spectrum available on the ISM bands (industrial, scientific, and medical purposes). Initially it started on the 2.4 GHz band and with the release of 802.11a it also used the 5.8GHz band. For the new standard in development, Wi-Fi 7, there are discussion in starting to use the 6GHz band to offer higher bandwidths that enable the data rates demanded by the users.

In the original release included three different PHYs: infrared (IR), frequency hopped spread spectrum (FHSS) and direct sequence spread spectrum (DSSS). Both radiofrequency PHYs work in the 2.4GHz frequency band, an ISM band for unlicensed spectrum. The one which had the most usage was the DSSS which was extended on the release 802.11b adding complementary code keying (CCK) and increasing the data rate to 11 Mbps.

Alternatively, to DSSS the 802.11a introduced a PHY based on OFDM in the 5GHz band with data rates up to 54Mbps. Despite its high performance the change of band slowed its implementation for two primary reasons. On one side, the band wasn´t allowed worldwide, initially was only allowed on select channels on the USA for non-military porpoises. On the other hand, the null compatibility with 802.11b in the 2.4 GHz band forced the devices to implement two radios if they wanted to keep the backwards compatibility with a popular implementation, increasing the requirements and consequently prices of the equipment.

In 2001 the use of OFDM in the 2.4 GHz was allowed and consequently the standard 802.11g was created, becoming fully adopted in 2003, which translates the 802.11a standard to the 2.4GHz band. Additionally, it incorporates fully backwards compatibility and interoperability with older devices using 802.11b, allowing the integration of new 802.11g devices in networks with pre-existing DSSS access points (AP) or the use of old user terminals with new AP incorporating the standard.

As stated before, the maximum data rate of the 802.11a and 802.11g was of 54Mpbs; to understand where it comes from, we can review the most important features of the standard. It used 52 populated subcarriers with 48 of those transporting data and the other pilots; considering the 20MHz band we assume a 312.5 kHz subcarrier spacing. The guard interval consists of 4µs, and the symbols modulations can vary from BPSK to 64QAM giving up to 6 bits modulated per symbol, also the forward error correction (FEC) rate varies between ½ and ¾. With this se can see the data rate calculation in the equation (2.1).

$$54\ Mbps = \frac{48\frac{data\ subcarriers}{symbol} * 6\frac{bits}{data\ subcarrier} * \frac{3}{4}}{4\frac{\mu s}{symbol}} \tag{2.1}$$

2.2. Wi-Fi 4 & 5

Eventually this data rates where lagging behind the needs of the market and other technologies, like the beforementioned Ethernet, thus an enhancement was necessary. The new standard was published on the release 802.11n also known as high throughput (HT) or Wi-Fi 4, defined for both the 5GHz and the 2.4GHz bands. In order to increase the data rate, the principal upgrades came from the use of MIMO introducing spatial diversity and the bandwidth increase to 40MHz, also the MAC layer received improvement to its efficiency and the guard interval can be shortened under favourable circumstances. Another benefit from the new standard is the increased robustness of the system with the introduction of techniques like the already mentioned MIMO, the space-time block coding (STBC) or low-density parity check (LDPC) codes.

To accommodate the mobile devices, which were experimenting a big growth inside the market during the years leading to the release of the 802.11n standard, the requirement of multiple antennas was only imposed to the access points (AP) and not at the user devices.

With all the improvements mentioned the new data rate achievable is calculated in (2.2) using the same procedure as (1). In this case we have 108 data subcarriers with the 40 MHz bandwidth, six bits per carrier with a 64QAM modulation, a 5/6 (FEC) rate, four independent data streams and a symbol duration of 3.6μs from the usage of the shorter guard interval. With all these characteristics the maximum data rate is 600Mbps.

$$600 \ Mbps = \frac{108\frac{data\ subcarriers}{symbol}*6\frac{bits}{data\ subcarrier}*\frac{5}{6}}{3.6\frac{\mu s}{symbol}} \cdot 4 \qquad (2.2)$$

The next evolution of the Wi-Fi standard came with the 802.11ac, also named very high throughput (VHT) or Wi-Fi 5, which was only defined for the 5GHz band. The general trend with the standard is a revision of the elements already present in the previous standards, simplifying the use of them and increasing the potential of them.

The principal methods to increase the throughput were the increase of the bandwidth with the introduction of 80MHz and 160MHz channels, the latter of them can be created using two non-contiguous 80MHz channels in an 80+80MHz configuration to increase the flexibility of the channel assignment. Many other improvements were introduced like the increase were the modulation with the introduction of 256QAM or the improvements to STBC, LDPC or transmit beamforming. Using the new values for the relevant parameters the maximum data rate is calculated in the equation (2.3) obtaining a value of 6.9Gbps, representing an increase over ten times over the previous standard.

$$6933.33 \ Mbps = \frac{468\frac{data\ subcarriers}{symbol}*8\frac{bits}{data\ subcarrier}*\frac{5}{6}}{3.6\frac{\mu s}{symbol}} \cdot 8 \qquad (2.3)$$

In terms of simplification, we can see examples in many different areas like STBC, LDPC, transmit beamforming and more. However, the most important change introduced in 802.11ac is the optional use of MU-MIMO in the downlink stream, allowing the AP to connect to multiple users simultaneously.

The PHY protocol data unit (PPDU) is the basic packet structure for the PHY layer. To maintain the interoperability between the different standards each one took into consideration the previous versions and adapted itself to not disturb the rest of them. To understand the preamble of each generation we need to study the evolution of them.

Initially on the 802.11a and 802.11g standards the preamble consisted of four fields: short training field (STF), long training field (LTF), signal field (SIG) and the data field. The STF occupies two OFDM symbols with a duration of 8μs and consist of ten repetitions of a short sequence; it is used for packet detection, automatic gain control (AGC) and an initial frequency offset estimation. The LTF occupies two OFDM symbols and contains two repetitions of a 3.2μs sequence prepended by a 1.6μs prefix; it is used to complement the frequency offset estimation and channel estimation. The SIG is contained in one OFDM symbol and transmit the information needed to decode the data field modulated using a BPSK modulation with 1/2 binary convolution code; it also contains the length of the packet which is used by the rest of the users to calculate the time the channel will remain occupied. In figure 2-1 we can see the structure of the PPDU for 802.11a/g.
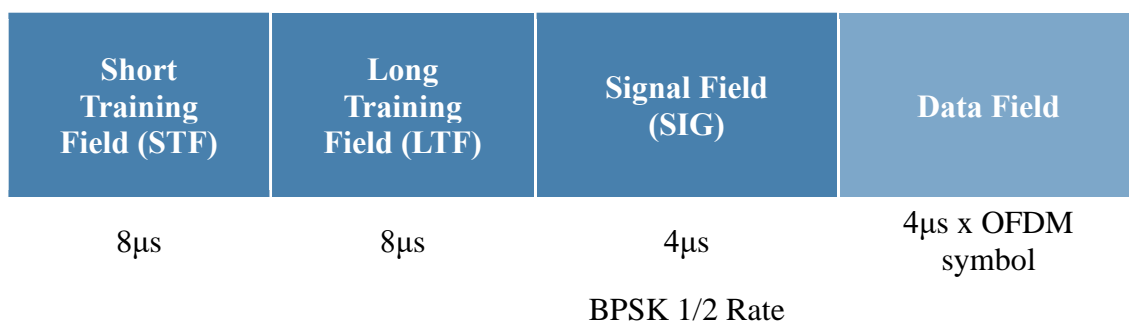
Short Training Field (STF)	Long Training Field (LTF)	Signal Field (SIG)	Data Field
8μs	8μs	4μs	4μs x OFDM symbol

BPSK 1/2 Rate

Figure 2-1 802.11a/g PPDU structure

In 802.11n we have two different preambles, the mixed format designed for interoperability with the previous standard and the greenfield format for networks without older devices or transmissions protected by the MAC layer protocol; the greenfield preamble is shorter than the mixed format increasing the performance, especially in applications with constant low value packets like VoIP. Due to the incompatibility with older devices and a performance increase not being big enough for the increased complexity its usage was few and far between.

The mixed format preamble to ensure interoperability starts with the same fields as the legacy devices, giving the older packets the capability of detecting the packet and calculating the time the channel will be occupied. When the transmitter incorporates more than one antenna we encounter two different potential issues, on one hand if we only

transmit from a single antenna we will have a reduction in output power if compared with a single antenna device; on the other hand, transmitting from all the antennas can potentially we can cause negative unintentional beamforming effects. The solution to the problem is transmitting the preamble through all the antennas applying a different cyclic shift to each one to mitigate the beamforming effects.

The legacy fields present almost no changes, the only ones are a small change on the L-STF power which in 802.11n is scaled to output a power of one instead of an equal power as the L-LTF like in 802.11a; the signal field fixes the rate to 6Mbps, and the length parameter is set to allow a correct duration estimation by a legacy device.

The first non-legacy field is the HT-SIG which contains two symbols with a total of 48 data bits modulated with 90 degrees shifted BPSK and encoded with 1/2 BCC. The shift in the modulation is introduced to allow the auto detection between a legacy packet and a HT packet. The HT-SIG field contains the necessary information to properly decode the encoded data.

The information firstly contains the modulations and coding schemes (MCS), that represent the modulation and coding scheme spatial streams used in the transmission of the packet according to the predefined table. The rest of the first symbol contains the bandwidth flag to differentiate between 20MHz and 40MHz transmission and the length of the packet, allowing packets of size up to 65535 bytes.

The second symbol contains flags related to transmit beamforming like the smoothing bit, that indicates if the channel estimation is done per-carrier, or the adjacent ones are taken into consideration. The not sounding bit indicates if the packet is a sounding packet used to estimate the channel state information. After a reserved bit we find the aggregation bit, indicating if the packet contains one mac protocol data unit (MPDU) or an aggregation of them. The next two bits indicate the dimensionality of the STBC. The next ones represent the FEC method, BCC or low-density parity check (LDPC), the usage of short guard interval and the number of extension spatial streams. The last bits incorporate the eight-bit cyclic redundancy check (CRC) and tail bits.

The previously defined fields need to be transmitted in 20MHz channels to ensure the interoperability with the older standards. Because of this when the communication

bandwidth presents a higher value the first parts of the preamble is repeated in the all the different subchannels occupying them and ensuring that no device interrupts the communication and allowing the 40MHz devices to combine both bands improving the detection of this fields. When replicating the 20MHz preamble to create the 40MHz output the higher band is rotated 90 degrees to reduce the peak to average power ratio (PAPR).

The next field is the HT-STF necessary to properly calculate the correct AGC values for the MIMO environment. This is necessary due to the cyclic shift restriction imposed by the legacy standard, creating a discrepancy between the cyclic shifts for the legacy part of the preamble and the new fields. The new AGC values are more accurate and allow to reduce the dynamic range on the analog digital converter (ADC). As a difference with the L-STF the HT-STF only contains one OFDM symbol, establishing a 4μs duration.

The last field of the preamble are the HT-LTF used to estimate the channel in the MIMO environment, it contains a 4μs OFDM symbol for each defined spatial stream except for three spatial streams where four symbols are transmitted to keep the added orthogonal mapping matrix non-complex. The mapping matrix multiply the sequence by +1 or -1. Also the cyclic shift from HT-STF is applied to the HT-LTF. The full HT PPDU structure can be found on the figure 2-2.

L-STF	L-LTF	L-SIG	HT - SIG	HT - STF	HT - LTF$_1$		HT - LTF$_N$	Data Field
8μs	8μs	4μs	8μs	4μs	4μs		4μs	4μs x OFDM symbol

BPSK 90º BPSK
1/2 Rate 1/2 Rate
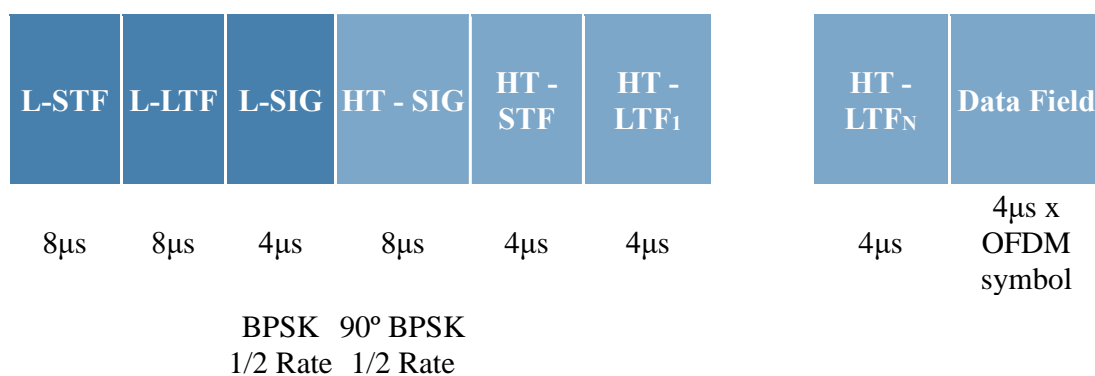
Figure 2-2 802.11n PPDU Mixed Format structure

The greenfield format follows a similar structure as the mixed one, starting with a STF field followed by a LTF, a SIG field and some optional additional LTF. The GF-HT-STF is created with a similar format to the HT-STF but the length is extended to 8μs matching the duration of the L-STF allowing an appropriate duration for start of packet

detection, AGC setting, frequency estimation and time synchronization. Thanks to the lack of interoperability the spreading matrix, derived from the beamforming or spatial expansion, can be applied to all the preamble, additionally we can use the long cyclic shift from HT-STF to all the entire preamble. This STF is enough to obtain all the information needed for the MIMO communication is attained and no other STF is needed.

The next field is the GF-HT-LTF which is created following the format of the HT-LTF, but the duration of the symbol is two times as long, occupying two OFDM symbols instead of one. The following field is the SIG field which contains the same information as the HT-SIG field. The last fields are the additional GF-HT-LTF found when the number of spatial streams is bigger than one. The added symbols are equal to the HT-LTF, and they follow the same norms as them. The full PPDU structure for the greenfield format can be found in the figure 2-3. In total the greenfield structure offers a 12μs reduction on the preamble duration.
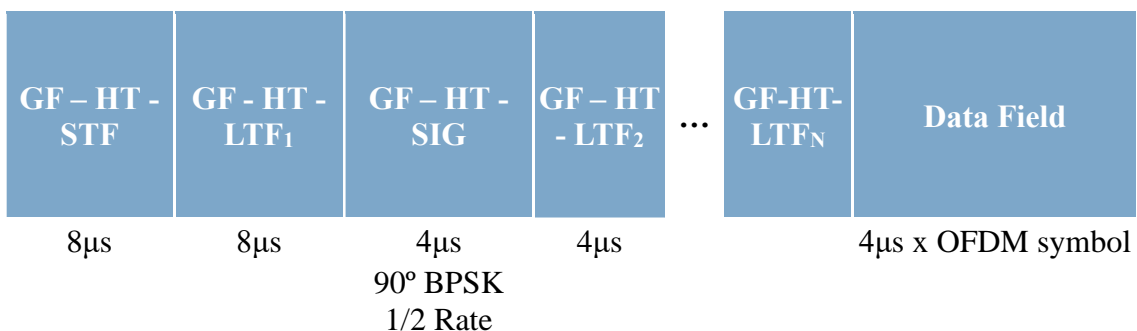

GF – HT - STF	GF - HT - LTF$_1$	GF – HT - SIG	GF – HT - LTF$_2$	...	GF-HT-LTF$_N$	Data Field
8μs	8μs	4μs 90º BPSK 1/2 Rate	4μs			4μs x OFDM symbol

Figure 2-3 802.11n PPDU Greenfield structure

In the 802.11ac there is only one preamble described, the mixed format one that keeps the devices interoperable with the older versions of the standard. Because of this requirement the first three fields are the legacy ones, L-STF, L-LTF, L-SIG; sharing the same requirements as the ones found in 802.11n. The only change comes from an extension of the cyclic shifts introduced to keep the interoperability, new values were needed to accommodate the new options given by the standard both in number of antennas and total channel bandwidth.

The first VHT field is the signal field A (VHT-SIG-A) which contains two OFDM symbols modulated with the same format as L-SIG. To facilitate the differentiation of the VHT PPDU from the other ones the first symbol is modulated with a normal BPSK and

the second one with a 90° shifted BPSK. To detect the Wi-Fi version we see the first field after the L-SIG field, if its modulated with 90° shifted BPSK, it is a HT packet; and if it is a BPSK we look for the following symbol determining if it is a legacy packet or a VHT depending on the phase of the BPSK.

The first symbol of VHT-SIG-A field starts with a two bits bandwidth field, to select from 20MHz to 160MHz channel, a reserved bit, an enable bit for STBC, the Group ID field, the NSTS field, the partial ID field, a power save enable bit and a last reserved field. The group ID field is used for MU communications indicating which MU group the communications belong based on the index of an internal table, reserving the values 0 and 63 for single user communications; each user table stores which position inside each group the user occupies. In the case of SU communications, the next field is a 3-bit NSTS field indicating how many spatial streams must be decoded and nine bits that include an abbreviation of the recipient ID. In MU cases this 12 bits contains four different NSTS field indicating to each user of group how many spatial streams must receive.

The second symbol of the VHT-SIG-A first two bits are related with the short GI with the first one acting as an enabler and the second one for disambiguation which is only used when $N_{SYM} mod\ 10 = 9$. The next two bits refer to the coding, with the first one selecting between BCC and LDPC and the second one indicating if the LDPC encoding has used an extra symbol. The next field indicates the MCS used with four bits, then a beamforming enable bit, a reserved bit, the eight-bit CRC and the tail bits.

A continuation, the VHT waveform is introduced with the VHT-STF and VHT-LTFs which are equivalent to the HT versions both in purpose and creation except for updated tables to incorporate the new options in terms of spatial streams and bandwidth. Lastly, we find a VHT-SIG-B field that contains information for the single user in MU packets. In SU cases it's kept maintaining a single format for all communications. When the bandwidth in bigger than 20MHz the field is repeated sequentially up to four times in 160MHz bandwidths allowing to average them getting processing gain. This field occupies an OFDM symbol and only contains the length of useful data. In SU is almost irrelevant but in MU can allow power saving, avoiding the reception of padding bits introduced to match another user. The 802.11ac PPDU structure can be seen in the figure 2-4
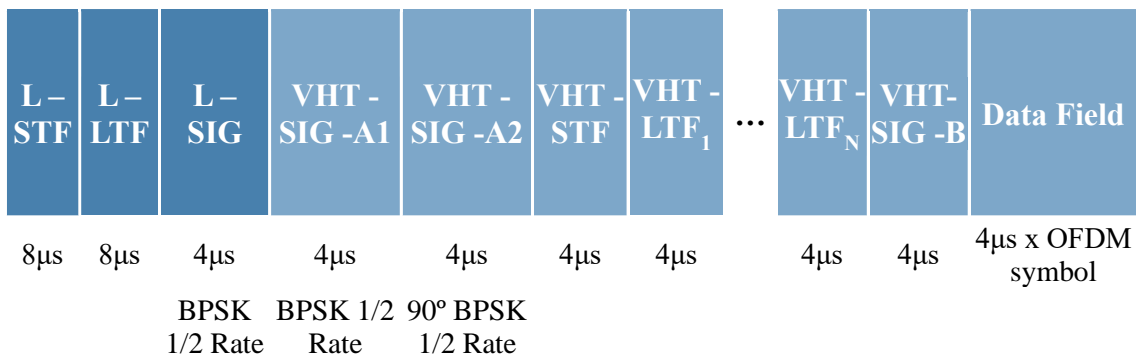
L – STF	L – LTF	L – SIG	VHT - SIG -A1	VHT - SIG -A2	VHT - STF	VHT - LTF$_1$	...	VHT - LTF$_N$	VHT- SIG -B	Data Field
8μs	8μs	4μs	4μs	4μs	4μs	4μs		4μs	4μs	4μs x OFDM symbol
			BPSK 1/2 Rate	BPSK 1/2 Rate	90º BPSK 1/2 Rate					

Figure 2-4 802.11ac PPDU structure

2.3. Wi-Fi 6

The 802.11ax, also known as Wi-Fi 6 and High Efficiency (HE) [3-5], is the last Wi-Fi standard fully released. Its design represented a revolution in how we perceive performance metrics. Previously the throughput was used as one of the most important parameters but the new environments present high density of users presenting a need for high number of AP and forcing the usage of partially overlapping channels. The overlap devalues the figure of aggregated throughput as a comparison measure, so instead the figure of merit should be the throughput density, which takes into consideration the area covered by the network when calculating the performance parameter.

The new environment also presents new challenges like a new primary source of signal degradation, the interferences between stations. To obtain the best performance out of the system is necessary not only to avoid the hidden nodes but also maximise the spatial reuse, maximizing the use of the available channels. Another change in the environment comes in the form of a new distribution of the traffic; between the rise of user generated content on social media and the services continually connected to storages on cloud. The new traffic structure is less asymmetrical increasing the stress in both the DL and UL channels. The new requirements introduce the need of MU-MIMO in both the DL channel that implemented optionally the feature on previous releases and in the UL channel where the timing requirements to implement such technique are more complex than anything encountered in previous standards.

Another challenge presented for the development of the standard was the presence of small packets, like the ones generated by instant messages, because in them the fixed packet overhead represents a huge portion of the time and resources needed to access the channel, significantly degrading the perceived performance in the application layer.

2.3.1. New Wi-Fi 6 features

The new version of the Wi-Fi standard presents in one hand an expansion on already existing characteristics to increase the data rate. On the other hand the inclusion of new features that help dealing with the new challenges presented to the standard, the high data density present at the networks. However, the bulk of changes are mainly present in the second part being demonstrated primarily by the low increase of the maximum throughput of only a 37% in comparison to 802.11ac that obtained a growth of more than 10 times the previous throughput.

In the second type of changes, we want to highlight the key feature of 802.11ax, the introduction of orthogonal frequency division multiple access (OFDMA) as a multiuser access technique. Since the introduction of large bandwidths such as 160MHz or 80+80MHz the system suffered from frequency selective interference, significantly impairing the practical data rates. OFDMA groups adjacent subcarriers in resource units (RU) and the senders can select the best RU to each receiver resulting in a better performance, both in signal to interference plus noise ratio (SINR) and throughput. Also permits the allocation of narrow channels to users with small amounts of data to transmit mitigating the effective data rate loss existing in smaller packets due to fix preambles.

OFDMA was already present in a commonly used communications standard the long-term evolution (LTE), included in the fourth generation of mobile communications. The implementation between the two standards differs on the allocation of resources, LTE presents a time-based allocation, allowing that various tones correspond to different user devices during one transmission time interval (TTI); meanwhile Wi-Fi is frame based,
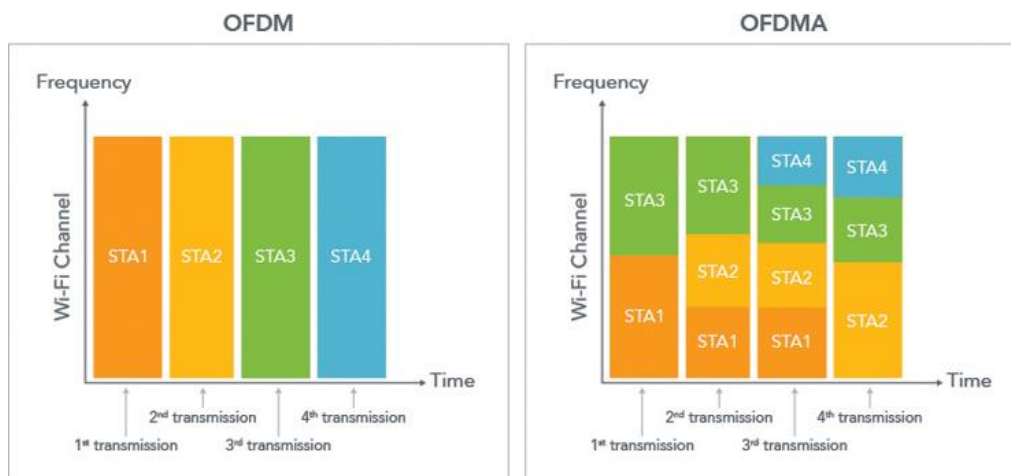

Figure 2-5 Comparison OFDM vs OFDMA [6]

allocating the tones to a group of users for the entire frame duration. A visual representation of the differences between the OFDM and OFDMA can be seen on the figure 2-5.

Aside from OFDMA other techniques are introduced to improve the performance in dense networks. Basic Service Set (BSS) colouring: the introduction of a unique code for each BSS in the PHY preambles helps identifying if the frame source comes from inside the BSS, intra-BSS, or from another BSS, inter-BSS. The code is selected randomly in the range 0-63 by the AP and in case of overlapping codes the BSS will start a colour change procedure notifying the other BSS of the change. It can also be used to save power, when identifying that a packet doesn't belong to your own BSS the user can discard it and stop listening.

Dual vector allocation network (NAV): In the older standards he BSS stablishes the channel as occupied when receiving either a frame preamble, an unknown signal 20dB above the minimum sensitivity or when indicated, the estimated time the channel will be occupied is stored in the NAV. This value will be increased when receiving a packet with a larger value than the current one but, it will not decrease when the new value is smaller. To reset the value the reception of a CF-End frame is needed. A problem of this implementation is that the user can receive a CF-End frame from an overlapping BSS without the knowledge of the AP, in this situation exist a high chance of collision because both the user and the station believe the network is free. The situation is more common in the dense networks considered for the Wi-Fi 6 standardization. To solve the issue two different NAV are implemented, one for the own BSS and another for the other BSS.

Quiet Time Period (QTP): To increase the efficiency of the network ad hoc and direct links can be used, but the possible interferences need to be controlled. The user can request the AP for a QTP, a periodic time interval reserved for ad hoc and direct links; if the request is accepted the AP forbids the other users to access the network during the QTP.

Dynamic sensitivity control (DSC) consists in adapting the sensitivity threshold to maximize the spatial reutilization. By increasing the threshold, we can reduce the amount of time being blocked by other BSS but at the same time we need a value high enough that we detect the communications inside our BSS.

Adjusting transmit power: To help balance collision avoidance and spatial reutilization the sensitivity changes are linked to a variation on the power transmitted. When you can receive with a higher sensitivity threshold means that the channel attenuation is low so to avoid interfering in the other users you reduce your transmitted power to compensate the lower attenuation on the channel, this adjustment can be done dynamically.

One clear use of the DSC is used during backoff times; the station will pause the backoff time while receiving a packet, but it can be restarted if it detects that it pertains to an interfering BSS and the received power is lower than the sensibility threshold; allowing to restart the backoff before the full packet is received. When the station obtains access to the channel the communication can be started with the transmitted power according to the sensitivity level stablished in each moment. This technique can be further improved in combination with the BSS colour, specifying which BSS can be occulted under the sensitivity and which need to be listened.

Preamble puncturing: In the previous standard each channel has a hierarchy of a primary channel, which has a 20MHz bandwidth, and multiple sequential secondary channels of different bandwidths. When transmitting in each channel the user utilizes them in order, starting with the primary channel and adding the next channel in line if it is available. This procedure gives the option of using channels of more than 20MHz when grouping the different channels. This sequential procedure stops the channel grouping when one secondary channel is occupied even if the next ones are available; this scenario becomes more common in dense networks because those secondary channels can occupy the primary channel of another BSS. The preamble puncturing techniques solves this issue by allowing the creation of high bandwidth channels with one or more occupied 20MHz channels; the puncturing consist of not transmitting the packet preamble in said channels and not allocating the RU belonging to these subchannels

A common feature of the modern AP is the creation of virtual AP, commonly used to deploy a guest Wi-Fi network, allowing a single AP to act as multiple BSS. While acting as different BSS some of its service information is the same between them but act as different entities communicating this information separately. The 802.11ax standard introduces the capability of sending the shared information simultaneously in a multiple

UNIVERSITAT
POLITÈCNICA
DE VALÈNCIA

_ TELECOM ESCUELA
TÉCNICA VLC SUPERIOR
DE INGENIERÍA DE
TELECOMUNICACIÓN

BSS; all the BSS inside the set share the same BSS colour and the frames from the set are considered intra-BSS frames.

The dense network environment offers to each user multiple possible base station to connect; to improve the performance of the network is necessary to distribute the load through the network, avoiding saturating nodes.

2.3.2. PHY: Modulation and frame format

The PHY layer for 802.11ax inherits multiple traits from the previously existing standards that must interoperate. It is based on a OFDM modulation with channel bandwidths of 20MHz, 40MHz, 80MHz, 80+80MHz and 160MHz. One of the most remarkable features is the addition of more subcarriers augmenting them by a factor of four and as consequence elongating the symbol duration by the same factor.

 This extension improved the performance of the two main characteristics of the standard, OFDMA and the uplink multiuser due to the increased resistance to inter-user jitter inherent in outdoor scenarios. Moreover, it provides a reduction in overhead by reducing the weight of the guard times. In the previous standards it was either 0.4μs or 0.8μs to the symbol duration of 3.2μs, representing 10% or 20% of the total transmission time; on the other hand, in the new standard the guard interval can be selected as 0.8μs, 1.6μs or 3.2μs and the symbol duration is 12.8μs, corresponding to 6%, 11% and 20% respectively. It also presents disadvantages like the reduced time to process the received packet and sending the response which impacts primarily the low-end devices. To alleviate the effects of it without reducing the channel usage efficiency it is allowed to introduce a packet extension with a variable length adjusted to the receiver and the packet sent.

The Wi-Fi 6 standard considers the use of the modulation formats present in the older standards: BPSK, 16QAM, 64QAM and 256QAM; and introduces a new level of modulation in the 1024QAM. In terms of code rate, we keep the previously available options of 1/2, 2/3, 3/4 and 5/6, also we see no expansion to the maximum number of spatial streams available that remain at 8. With all the aforementioned characteristics at their highest value we can calculate the throughput using equation (2.4), obtaining the result of 9.6Gbps.

$$9607.8 \ Mbps = \frac{1960\frac{data\ subcarriers}{symbol}*10\frac{bits}{data\ subcarrier}*\frac{5}{6}}{13.6\frac{\mu s}{symbol}} \cdot 8 \qquad (2.4)$$

In the other end of the performance metrics, we find the inclusion of a dual carrier modulation which allows the transmission of the same information on two tones separated far apart in terms of frequency. The redundancy introduced with the modulation allows for a more reliable and robust communication at the expense of transmitting the same data twice, halving the throughput, reason to allow it to be used only with the most robust MCS.

2.3.3. OFDMA

OFDMA allows to allocate the resources both in time and frequency slots. Time wise to maintain the interoperability with older devices the assignments are frame based, meaning that one frame can assign different RU to different users but all of them must share the same duration. Frequency wise the different users can be given RU of different sizes, with the accepted values of 26, 52, 106, 242, 484, 996 and 2x996 subcarriers. The 242 tones RU is equivalent to a full 20MHz channel and each RU that doubles it correlates with the higher bandwidth channels. Each resource unit can be divided into two of the previous one except the 242 subcarriers that is divided into two 106 and one 26 subcarriers RU.

The OFDMA technique can be used in conjunction with MU-MIMO but it is limited to RU of at least 106 subcarriers. With the MU-MIMO we can allocate up to eight users to each RU and each individual user can use up to four spatial streams respecting the maximum number of spatial streams available.

The downlink OFMA communications are organized using the HE-SIG-B field on the preamble. It contains the RU allocation map and the per-user information indicating which RU are allocated to the station and the transmission parameters allocated to it. The uplink OFDMA organization is a more complex matter, specially thanks to the timing synchronization. Maintaining strict time synchronization with clocks is unviable due the clock drift and as consequence a new type of con control frame is created to resolve the problem, the trigger frame. This frame specifies the common parameters for the upcoming transmission that is performed immediately following the trigger frame. The frame contains information about the common parameters, the allocation of RU to

different users and the specific transmission parameters for each user. If preparing the transmission costs more than the time between messages the trigger frame can be padded to extend its duration and give enough times to the stations to prepare the upcoming transmission.

The standard defines a power pre-correction mechanism to ensure the correct received power from each user. The access point sends to the stations on the trigger frame the current transmit power and the expected received signal strength, with these values the users can calculate the pathloss and with it the necessary transmit power to obtain the requested power at the access point. In the uplink communications the MCS is dictated by the access point, not the user and to allow a correct assignment of the parameter the user includes its power headroom, the margin between the maximum transmit power and the current transmit power for the assigned MCS. The stations also inform the access point of the current amount of buffered data to be transported, allowing the access point to allocate an RU only to the users that have data to transmit. The AP indicates the users whether it shall perform carrier sensing, if the users is indicated to perform carrier sensing it will perform both, virtual and physical, at least in the 20MHz channels containing the subcarriers allocated to the user. If the physical carrier sense indicates that some of the tones are not idle the transmission must be cancelled; the virtual carrier sense can be occasionally bypassed if it has been set by a neighbour of the same BSS or the transmission consists of an ACK or block ACK with a duration shorter than a predetermined value. When the transmission time is longer than the one indicated in the trigger frame it is cancelled.

The UL MU transmission can be scheduled during the downlink transmissions either by including the trigger packet in the DL communication or by including information in the DL PPDU MAC header, which can also be used to acknowledge the uplink transmission during a downlink transmission. Combining the two uses we can organize a cascading sequence of transmissions where the UL and DL alternate inside the same TXOP, those communications can be single user or multiuser.

2.3.4. Preamble

The HE standard defines four different types of PPDU, single user PPDU (HE-SU-PPDU), extended range single user PPDU (HE-ER-SU-PPDU), multiuser (HE-MU-

UNIVERSITAT
POLITÈCNICA
DE VALÈNCIA

_ TELECOM ESCUELA
TÉCNICA VLC SUPERIOR
DE INGENIERÍA DE
TELECOMUNICACIÓN

PPDU) and trigger based (HE-TB-PPDU). They are based on a common base with special fields added to address the special needs of each type. The MU packets are common, describing which tones belong to each user, in the uplink all the transmitters is sent the same preamble with a different data fields.

To maintain the interoperability with the legacy standards the preamble starts with the legacy format, with two training fields and a signal field, following the structure of the past standards. Furthermore, to differentiate between the past standards and the HE standard it repeats the L-SIG field.

The first HE fields on the preamble is the HE-SIG-A which carries the information needed to interpret the packet. It is contained in two OFDM symbols, a duration of 8μs, except on HE-ER-SU-PPDU where it is repeated lasting twice as long. Furthermore, it has different structures for the different packet structures.

In the HE-SU-PPDU and HE-ER-SU-PPDU the HE-SIG-A field is shared; the first of the two symbols start with a first bit used to differentiate between them and the HE-TB-PPDU. Following it there are a bit to indicate if there is a change on the spatial modulation between, HE fields and non-HE fields. The next field determines if is an uplink or downlink communication, and after it we have the MCS field. After it we find the dual carrier modulation flag bit, the bandwidth field, the short duration guard interval flag and the number of spatial streams field. This last field has two possible meanings depending on the Doppler field, if it is zero, it means how many spatial streams are used up to eight, with limited values for ER-HE-PPDU; if the value is 0, the first two bits indicate the number of antennas and the last one indicates the periodicity of the midamble.

The midamble is a repetition of the HE-LTF field in the middle of the packet to allow channel estimation continuously during the packet duration. This is necessary to improve the performance in rapidly changing environments, especially common in scenarios with fast moving object producing Doppler effects.

The second symbol starts with the transmission opportunity (TXOP) field where it indicates in the first bit the units of measurement and the next six the value of it. Then there are flags for the code used, the presence of the LDPC extra symbol, the STBC configuration, the usage of beamforming, pre-FEC padding factor, the packet extension

disambiguity, a reserved bit and the Doppler field. The last fields are CRC and tail bits. The Doppler bit is 1 either if the midamble is present and the number of OFDM symbols is longer than the specified midamble periodicity, or the midamble is not present, it is recommended and the number of OFDM symbols is shorter than the announced midamble periodicity.

The HE-SIG-A field for a HE-MU-PPDU starts with a bit indicating the direction of the communication either uplink or downlink. Then we find bits regarding the HE-SIG-B field, exclusive of the HE-MU-PPDU, specifically the MCS used to encode it using three bits and the usage of DCM modulation. The next six bits indicate the BSS colour, the following four the spatial reuse and three bits to establish the bandwidth and puncturing. The subsequent field occupies four bits and indicates either the number of users or the number of OFDM symbols occupied by the HE-SIG-B field depending on the value of the Common field in HE-SIG-B, after it we move to a bit indicating the presence of said field on the HE-SIG-B. The first symbol finalises with the field indicating the guard interval size and the Doppler field.

The second symbol is composed of the TXOP field, occupying seven bits, a reserved bit, a three-bit long field indicating the number of HE.LTF symbols and the midamble periodicity, the bit indicating the presence of the LDPC extra symbol, the STBC configuration bit, the pre-FEC padding factor, the PE disambiguity and finalises with the CRC and the tail bits.

The HE-SIG-B field is used to provide the necessary signaling information to allow each STA to look up the corresponding resources allocated to them, it includes the OFDMA and MU-MIMO allocation. It can optionally contain a common field indicating information directed to all the users. The information in the common field is divided in two subfields the first of them indicates for each 20MHz subchannel the distribution of the RU in both size and location inside the spectrum; the subfield is repeated with higher bandwidths covering each subchannel separately. The second field, only present with bandwidths higher than 40MHz, determines if a user is in the central 26-tone RU. The user field incorporates the information necessary to decode the payload and is different for non-MU-MIMO and MU-MIMO. The first of them incorporates the station ID, the number of spatial streams, the beamforming flag, the MCS, the DCM bit and the coding.

For MU we encounter the station ID, the spatial configuration which indicates how many spatial streams are allocated for each user, the MCS and the coding.

The preamble for the HE-TB-PPDU starts with the same format bit as the HE-SU-PPDU, to differentiate between them and the BSS colour field. Next, we find four different fields, four-bit long indicating the spatial reutilization of the different bands inside the bandwidth. The first symbol finishes with a reserved bit and the bandwidth field. The second symbol is only occupied with the TXOP field, and the CRC and tail bits at the end. The middle of the symbol is reserved.

The next fields in the HE-PPDU are the training fields HE-STF and HE-LTF. The function of them is to adjust the settings of the automatic gain control for MIMO and channel estimation respectively. The first of them, HE-STF duration in one OFDM symbol and is doubled for the HE-TB-PPDU. The HE-LTF duration is one symbol for each spatial stream supported in the communication, counting all the users in the system. To create the waveforms the procedure followed is like the previous standards with an updated tables to accommodate the new options.

2.4. Wi-Fi 7

The process of standardization of Wi-Fi 6 finished in 2019 and the discussions for the new version started in that same year. The new standard needed to respond to the higher necessities in terms of throughout and latency generated by the new applications like 4k or 8k video streaming, virtual reality, augmented reality, cloud computing and many more. The Wi-Fi 6 has focused in the density of data transmitted increasing the performance greatly in networks with many users but the increase in throughput has been small compared to previous realises. The Wi-Fi 7, also known as 802.11be [7-10] or extremely high throughput (EHT) is proposed to reach a throughput of at least 30Gbps in the frequency bands between 1 and 7.25GHz while keeping the backwards compatibility.

Between the multiple proposed changes that are being discussed we can find the proposal of increasing the bandwidth up to 320 MHz with new options for non-contiguous channels. Additionally, the standard also intends to improve the throughput with the usage of a higher order of modulation in the 4096QAM which will be available when the channel conditions are very good. In the realm of efficiency two changes proposed are the possibility of assigning a single user multiple RUs increasing the flexibility when

assigning resources to the users and the introduction of new preamble formats and puncturing mechanisms. The preamble also pretends to future proofing the compatibility introducing a version field allowing the differentiation of new versions without introducing elaborated techniques like the old standards that relied on constellation shifts, repeating fields and other techniques.

In terms of MAC enhancements, we can look into the proposed use of multi-link operation allowing the simultaneous connexions at the different frequency bands available to Wi-Fi in 2,4, 5 and 6 GHz. This allows an increase in total bandwidth available and due to it the increase of the reliability and throughput of the system. To improve the reliability in EHT the implementation of hybrid automatic repeat request (HARQ) as the retransmission mechanism, allowing the soft combination of different retransmissions or the retransmission of additional parity improving the likelihood of correct decoding of the signal.

Other fields of discussion are the improvements to the channel state information (CSI) acquisition needed to support the proposed new maximum of 16 antennas for MIMO. Another proposed feature that will create constraints in the coordination overhead is the multi-access point coordination which shares data and control information to coordinate the different AP that reach one user allowing the techniques of coordinated spatial reuse (CSR), coordinated frequency division multiple access (C-OFDMA), coordinated beamforming (CBF) and joint transmission (JXT). This new technique will provide an improvement to the performance at the cost of high requirements for information exchange, phase and time synchronization and resource allocation, if any of them fail the result may provide a worse performance that not applying them at all.

2.5. Summary of Wi-Fi standards characteristics

As a summary a table incorporating the principal characteristics of each Wi-Fi standard can be seen on the table 1.

Table 1: Summary principal Wi-Fi standards characteristics

	802.11a & 802.11g	802.11n, HT	802.11ac, VHT	802.11ax, HE	802.11be, EHT
Frequency bands	5 GHz (a) | 2.4 GHz (g)	2.4 & 5 GHz	5 GHz	2.4, 5 & 6 GHz	2.4, 5& 6 GHz
Maximum bit rate	54 Mbps	600 Mbps	6.9 Gbps	9.6 Gbps	46 Gbps
Channel Bandwidth	20 MHz	20 / 40 MHz	20 / 40 / 80 / 160 MHz	20 / 40 / 80 / 160 MHz	20 / 40 / 80 / 160 / 320 MHz
Multiplexing scheme	OFDM	OFDM	OFDM	OFDMA	OFDMA
Maximum subcarrier modulations	64QAM	64QAM	256QAM	1024QAM	4096QAM
FEC rate	1/2, 2/3, 3/4	1/2, 2/3, 3/4, 5/6	1/2, 2/3, 3/4, 5/6	1/2, 2/3, 3/4, 5/6	1/2, 2/3, 3/4, 5/6
Subcarrier spacing	312.5 kHz	312.5 kHz	312.5 kHz	78.125 kHz	78.125 kHz
Symbol duration	12.8/6.4/3.2 µs	3.2 µs	3.2 µs	12.8 µs	12.8 µs
Guard interval (GI)	3.2/1.6/0.8 µs	0.4 / 0.8 µs	0.4 / 0.8 µs	0.8/1.6/3.2 µs	0.8/1.6/3.2 µs
Nss	1	4	8	8	8
Multiuser	No	No	MU-MIMO in DL	MU-MIMO & OFDMA	MU-MIMO & OFDMA

UNIVERSITAT
POLITÈCNICA
DE VALÈNCIA

_ **TELECOM** ESCUELA
TÉCNICA **VLC** SUPERIOR
DE INGENIERÍA DE
TELECOMUNICACIÓN

3. MU-MIMO

3.1. MIMO

The traditional systems used one antenna at the receiver and one antenna at the transmitter, creating a single input single output (SISO) configuration. This system is simple but limited in its capabilities. To enhance the system the introduction of more antennas is needed creating either SIMO (single input multiple output), MISO (multiple input single output) or MIMO (multiple input multiple output) systems. These systems exploit the variety of paths the signal can take from the transmitter to the receiver to enhance the performance, using the multiple paths between different antennas to create individual data streams creating spatial diversity. The additional data paths can be used to carry the same information, thus increasing the redundancy and consequently the reliability of the system, or different information increasing the throughput without increasing the bandwidth of the system therefore increasing the spectral efficiency of the system.

The introduction of antennas creates both an opportunity to improve the system and a problem, the different signals from each antenna will be received at the system so is necessary to introduce a method of eliminating the signals from different data streams. Thanks to the different paths taken by each signal we will be able to separate them with the correct receiver and potentially a precoder.

3.1.1. System model

The system is composed of a transmitter with N_{tx} antennas and a receiver with N_{rx} antennas. On a traditional SISO system, the received signal y can be calculated as the transmit signal x going through the impulse response of the channel h plus the added noise n as seen on equation (3.1). For the MIMO system we can utilize the same structure but instead of having a received signal we have a vector of the received signals at each antenna at the receiver $\boldsymbol{y}$, the transmitted signal is the vector containing the transmitted signals at each transmit antenna $\boldsymbol{x}$, the channel response is a matrix indicating the responses from each transmit antenna to each receive antenna **H,** as seen on the equation (3.2).

$$y = hx + n \qquad\qquad (3.1)$$

$$\begin{bmatrix} y_1 \\ y_2 \\ \dots \\ y_{N_{rx}} \end{bmatrix} = \begin{bmatrix} h_{1,1} & h_{2,1} & \dots & h_{N_{tx},1} \\ h_{1,2} & h_{2,2} & \dots & h_{N_{tx},1} \\ \dots & \dots & \dots & \dots \\ h_{1,N_{rx}} & h_{2,N_{rx}} & \dots & h_{N_{tx},N_{rx}} \end{bmatrix} \begin{bmatrix} x_1 \\ x_2 \\ \dots \\ x_{N_{tx}} \end{bmatrix} + \begin{bmatrix} n_1 \\ n_2 \\ \dots \\ n_{N_{rx}} \end{bmatrix} \rightarrow \boldsymbol{y} = \boldsymbol{Hx} + \boldsymbol{n} \qquad (3.2)$$

3.1.2. Zero Forcing decoder

The simplest way of separating the different data streams in the MIMO system is introducing at the receiver a zero forcing (ZF) decoder which cancels the channel effect by multiplying the received signal by the invers of the channel matrix $\boldsymbol{H}^{-1}$. Because not every matrix can be inverted instead of the pure invers of the matrix the Moore-Penrose pseudoinverse $\boldsymbol{H}^+$ [11] is used, expressed in the equation (3.3) where the H^H indicates the Hermitian matrix, the conjugated transpose. When the invers of a matrix exists, it is the result of the pseudoinverse. Applying the pseudoinverse, we can separate the data streams as the equation (3.4) indicates, obtaining the received vector $\hat{\boldsymbol{x}}_{ZF}$ compounded of the independent transmitted vectors plus the noise.

$$\boldsymbol{H}^+ = (\boldsymbol{H}^H \boldsymbol{H})^{-1} \boldsymbol{H}^H \qquad (3.3)$$

$$\boldsymbol{H}^+ \boldsymbol{y} = \boldsymbol{H}^+ \boldsymbol{Hx} + \boldsymbol{H}^+ \boldsymbol{n} \rightarrow \hat{\boldsymbol{x}}_{ZF} = \boldsymbol{x} + \boldsymbol{H}^+ \boldsymbol{n} \qquad (3.4)$$

3.1.3. MMSE decoder

One of the principal problems of the zero forcing decoder comes from ignoring the effect of the noise on the received signal, creating a scenario where in cases with low signal to noise ratio (SNR) the decoder matrix can potentially amplify the effect of it over the received signal reducing the performance. To solve the issue the minimum mean square error (MMSE) decoder [12] was create, modifying the ZF precoder to take into consideration the effect of the noise in the received signal, obtaining the decoder matrix $\boldsymbol{H}^+_{MMSE}$ as shown in the equation (3.5) where **I** indicates an identity matrix. Using it we can obtain the decoded signal $\hat{\boldsymbol{x}}_{MMSE}$ as indicated in (3.6).

$$\boldsymbol{H}^+_{MMSE} = \left[\frac{1}{SNR} \boldsymbol{I} + \boldsymbol{H}^H \boldsymbol{H} \right]^{-1} \boldsymbol{H}^H \qquad (3.5)$$

$$\boldsymbol{H}^+_{MMSE} \boldsymbol{y} = \hat{\boldsymbol{x}}_{MMSE} = \boldsymbol{H}^+_{MMSE} \boldsymbol{Hx} + \boldsymbol{H}^+ \boldsymbol{n} \qquad (3.6)$$

Can be seen that when the signal to noise ratio grows it's influence over the matrix reduces and solution approximates to the ZF solution, this method offers a higher performance in low SNR scenarios at the cost of a complexity cost.

3.1.4. SVD decomposition

An alternative method of separating the different channels is using the SVD decomposition [13] of the channel matrix. The SVD decomposition separates the matrix in three new matrixes, $H = USV^H$. The matrixes $\mathbf{U}$ and $\mathbf{V}$ are unitary matrixes and $\mathbf{S}$ is a diagonal matrix composed of the singular values of the original matrix. Using this scheme, we will precode the data with the matrix $\mathbf{V}$ and we will use the matrix U^H as the decoder matrix, separating the signals as following the process of the equation (3.7) obtaining the decoded signal. Because the innate properties of the matrixes we can assess that $\mathbf{UU}^H = I$ and $\mathbf{VV}^H = I.$

$$U^H y = U^H HVx + U^H n \rightarrow \hat{x}_{SVD} = U^H USV^H V x + U^H n = Sx + U^H n \qquad (3.7)$$

Because the matrix $\mathbf{S}$ is a diagonal matrix this method ensures that the different data streams are separated.

3.2. MU-MIMO

Just like OFDM introduced a multiplexing mechanism to allow a multiuser communication in the form of OFDMA utilizing the frequency diversity, the MIMO techniques can be expanded into a multiuser communication technique utilizing the spatial diversity created by the multiple antennas. The MIMO techniques create multiple spatial streams allowing to transmit multiple independent data streams, these streams can be divided to the different users creating the MU-MIMO communication. These systems normally are composed of a central node with higher capabilities and multiple smaller nodes with fewer antennas, coinciding with the typical Wi-Fi network, with one access point with multiple antennas and users with only one or two antennas. This study is focussed on the downlink communication.

3.2.1. System model

The new system model in a MU-MIMO is like the one used in single user MIMO, it consists of a transmitter with N_{tx} antennas transmitting to k users with N_j antennas each and a total of N_{rx} antennas. The transmitter utilizes a precoding matrix $\mathbf{P}$ and the receiver a detector matrix $\mathbf{M}$. The signal received at each user y_j can be calculated by using the expression from the equation (3.8) and the detected signal $\hat{x}_j$ using the expression from

UNIVERSITAT
POLITÈCNICA
DE VALÈNCIA

_ TELECOM ESCUELA
TÉCNICA **VLC** SUPERIOR
DE INGENIERÍA DE
TELECOMUNICACIÓN

the equation (3.9). These equations show three different components to the received signal, firstly the desirable information formed with the signal sent the specific user going through the channel; secondly, we find the inferring signal composed by the information sent to other users after it propagated through the channel; and lastly the added white noise.

$$y_j = H_j P_j x_j + H_j \sum_{k=1;k\neq j}^{K} P_k x_k + n_j \qquad (3.8)$$

$$\hat{x}_j = M_j H_j P_j x_j + M_j H_j \sum_{k=1;k\neq j}^{K} P_k x_k + M_j n_j \qquad (3.9)$$

3.2.2. Precoder design

The design of the precoder is the most important part of the downlink MU-MIMO communications because the transmitter is the only element with full information of the system thus is essential that it separates the information in a way that each user can identify its information without interference from other user's information. Looking at the system model we have that the interferences comes from the middle element, so we need to design of precoding matrix **P** so that $H_j P_k = 0 \ \forall j \neq k$.

3.2.3. Zero Forcing precoder

The simplest way of precoding the signal is selecting the pseudoinverse of the channel matrix as the precoding matrix [14], following the scheme of the homonymous linear detector. The channel invers is calculated with the expression from equation (3.3), but to calculate the precoding matrix a normalization of the resultant matrix is done to avoid affecting the transmitted power. The normalization can be done under two different constraints, total transmit power where the normalization occurs over the whole channel matrix (3.10); or user power constraint where the normalization is done user by user, limiting the total power transmitted to each user (3.11). Using these precoders the total data rate attainable is calculated using the expression (3.12), where L_{pl_j} indicates the propagation losses experimented by the signal and σ_n^2 represents the noise power.

$$P_{ZF_{norm}} = \frac{P_{ZF}}{\sqrt{trace(P_{ZF}P_{ZF}{}^H)}} \qquad (3.10)$$

$$P_{ZF_{j_{norm}}} = \frac{P_{ZF_j}}{\sqrt{trace\left(P_{ZF_j}P_{ZF_j}{}^H\right)}} \rightarrow P_{ZF_{norm}} = [P_{ZF_{1_{norm}}}, \dots, P_{ZF_{K_{norm}}}] \qquad (3.11)$$

UNIVERSITAT
POLITÈCNICA
DE VALÈNCIA

_ **TELECOM** ESCUELA
TÉCNICA **VLC** SUPERIOR
DE INGENIERÍA DE
TELECOMUNICACIÓN

$$R_{ZF} = \sum_{j=1}^{K} log_2 \left(1 + \frac{\frac{P_{Tx_j}}{L_{pl_j}\sigma_n^2}}{\sqrt{trace\left(P_{ZF_{j_{norm}}} * P_{ZF_{j_{norm}}}^H\right)}} \right) \qquad (3.12)$$

3.2.4. MMSE Precoder

Following the linear detector reasonings, the zero forcing precoder doesn´t take into consideration the added noise thus providing bad performances at low SNR values. Similarly to the linear detector case we can calculate the precoder with the expression (3.5) obtaining a better performance in scenarios with low SNR and the same behavior when the SNR is high. After the normalization process (3.13) we obtain the precoding matrix. The maximum data rate can be calculated with the equation (3.14).

$$P_{MMSE_{norm}} = \frac{P_{MMSE}}{\sqrt{trace(P_{MMSE} * P_{MMSE}^H)}} \qquad (3.13)$$

$$R_{MMSE} = log_2 \left| I + SNR \cdot H * P_{MSSE_{norm}} * P_{MMSE_{norm}}^H * H^H \right| \qquad (3.14)$$

3.2.5. Block diagonalization

The ZF and MMSE precoders offer a low performance when the number of antennas at the receivers are more than one, and as a solution one of the most used precoders is the block diagonalization [15]. This precoder similarly to the zero forcing method focusses on canceling the channel effects without incorporating into it the effect of the noise in the signal. This precoder separates operates in two steps, the first one cancels the multiuser interference and the second one separates the subchannels.

For the first step we need to create the modified channel matrix with all the interfering channels to the desired user (3.15) which rank is equal to $\tilde{L}_j = rank(\widetilde{H}_j)$, then we do the SVD decomposition of it (3.16) giving us as a result $\widetilde{U}_J$, $\widetilde{S}_J$ and $\widetilde{V}_J$. For this step on $\widetilde{V}_J$ matters because the last $N_{tx} - \tilde{L}_j$ columns of the matrix, $\widetilde{V}_j^{(0)}$, contain an orthogonal base for the null space of H_j meaning that $H_j\widetilde{V}_j^{(0)}$ gives the single user channel for the user.

$$\widetilde{H}_j = [H_1; \dots H_{j-1}; \dots; H_{j+1}; \dots _K] \qquad (3.15)$$

$$\widetilde{H}_j = \widetilde{U}_j\tilde{S}_j \left[\widetilde{V}_j^{(1)}, \widetilde{V}_j^{(0)}\right]^H \qquad (3.16)$$

The second steps take the single channel user and applies again the SVD decomposition of it (3.17). Repeating the process of the SVD decoder explained in the previous section we use the matrix $M_j = U_j^{(b)^H}$ for the decoding of the signal on the receiver and for the transmitter the precoding matrix P_j follows the expression (3.18), with the use of these matrixes the decoded signal is as (3.19) exemplifies, obtaining a result where the transmitted signal is multiplied only by the diagonal matrix $S_j^{(b)}$ keeping the different subchannels separated and without interference from other users.

$$H_j \widetilde{V}_j^{(0)} = U_j^{(b)} S_j^{(b)} V_j^{(b)^H} \tag{3.17}$$

$$P_j = \widetilde{V}_j^{(0)} V_j^{(b)} \tag{3.18}$$

$$\widehat{x}_j = M_j y_j = U_j^{(b)^H} H_j \widetilde{V}_j^{(0)} V_j^{(b)} x_j + U_j^{(b)^H} H_j \sum_{k=1;k\neq j}^{K} \widetilde{V}_j^{(0)} V_j^{(b)} x_k + U_j^{(b)^H} n_j =$$
$$U_j^{(b)^H} U_j^{(b)} S_j^{(b)} V_j^{(b)^H} V_j^{(b)} x_j + U_j^{(b)^H} n_j = S_j^{(b)} x_j + U_j^{(b)^H} n_j \tag{3.19}$$

With all these parameters we can calculate the sum rate of the system as (3.20) where σ_ω^2 signifies the noise power and Φ_j the power allocation matrix which indicates how much power is assigned to each signal under the constraint that $\sum_{j=1}^{K} Tr(\Phi_j) \leq P_{total}$. The power distribution can be calculated under different metrics but in relation to the data rate the waterfilling solution offers the optimal solution.

$$R_{BD} = max \sum_{j=1}^{K} log_2 \left| I + \frac{\left(S_j^{(b)}\right)^2 \Phi_j}{\sigma_\omega^2} \right| \tag{3.20}$$

The equations (3.21-3.22) contain the consolidated values of the precode and decode matrixes with all the subchannels taken into consideration.

$$P_{BD} = \left[\widetilde{V}_1^{(0)} V_1^{(b)}, \dots, \widetilde{V}_K^{(0)} V_K^{(b)} \right] \Phi^{\frac{1}{2}} \tag{3.21}$$

$$M_{BD} = diag\{U_1^{(b)^H}, \dots, U_K^{(b)^H}\} \tag{3.22}$$

Waterfilling [16] is a technique that allows the solution of multiple engineering problems based on constrained optimization, like the power allocation in a multichannel communication. Its name comes from the visual representation of the technique, pouring water over the surface given by the invers of the channel response. The solution of

UNIVERSITAT
POLITÈCNICA
DE VALÈNCIA

_TELECOM ESCUELA
TÉCNICA VLC SUPERIOR
DE INGENIERÍA DE
TELECOMUNICACIÓN

waterfilling problems is a deeply studied field with multiple methods to solve the problem, both analytical and numerical.

A simple visualization of a waterfilling solution is shown on figure 3-1, where a group of subchannels with different channel responses are distributed a set amount of power. In this example the problem only presents only one water level and one constraint, reducing the problem to the simplest expression. To solve the it the process obtains firstly the invers of the subchannel gain λ_n^{-1} is calculated; then a water level μ is set to a point where the sum of power given to each channel doesn't exceed the total power constraint. The power then is assigned to each subchannel until they reach the water level, if any channel has a λ_n^{-1} such that the waterlevel is at a lower value the subchannel won´t have any assigned power and no transmission will occur at that channel.
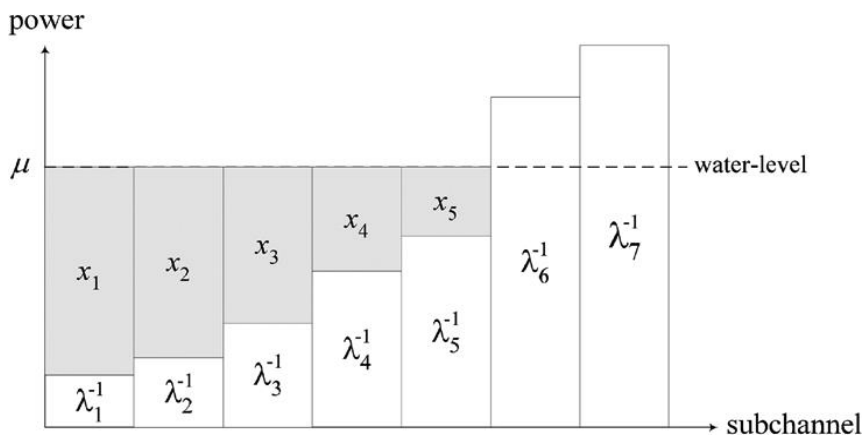

Figure 3-1 Visual representation of a waterfilling solution [16]

3.2.6. Generalized Zero Forcing Channel Inversion

An alternative to the block diagonalization comes from the generalized zero forcing channel inversion (GZI), which utilizes an alternative method to obtain the same result as BD with a lower complexity. This method starts generating the channel matrix pseudoinverse and separating the values corresponding to each user as seen on equation (3.23).

$$\widehat{H} = H^H(HH^H)^{-1} = [\widehat{H}_1, \widehat{H}_2, \dots, \widehat{H}_K] \tag{3.23}$$

From this point instead of utilizing the SVD decomposition as BD it utilizes the QR decomposition of the matrix $\widehat{H}_j$ obtaining $\widehat{H}_j = \widehat{Q}_j \widehat{R}_j$. In this decomposition the

matrix $\widehat{R}_j$ is a $N_j x N_j$ upper triangular matrix and $\widehat{Q}_j$ is an $N_t x N_j$ matrix whose columns form an orthonormal base for $\widehat{H}_j$. Combining the results from (3.15) and (3.23) we can deduce that $\widetilde{H}_j\widehat{H}_j = 0$, and after applying the QR decomposition to $\widehat{H}_j$ and the fact that $\widehat{R}_j$ is invertible we can reduce the expression to $\widetilde{H}_j \widehat{Q}_j = 0$. With this result we can see how $\widehat{Q}_j$ constitutes an orthonormal base for the null space of $\widetilde{H}_j$, obtaining the same result as the first SVD decomposition of the BD method.

Then applying the second BD step we obtain the same results so we can apply the same logic to the decomposition $H_j \widehat{Q}_j = U_j^{(z)}S_j^{(z)}V_j^{(z)H}$ and utilize the Hermitian of the first component as the decoder matrix and the third component as part of the precoder, obtaining (3.24, 3.25). As mentioned before this result is identical to the BD in terms of performance but its improvement comes from the fact that the QR decomposition realized in this process is simpler than the SVD decomposition needed by the BD.

$$P_j = \widehat{Q}_j V_j^{(z)} \rightarrow P_{GZI} = \left[\widehat{Q}_1 V_1^{(z)}, \dots, \widehat{Q}_K V_K^{(z)}\right] \boldsymbol{\Phi}^{\frac{1}{2}} \qquad (3.24)$$

$$M_j = U_j^{(z)H} \rightarrow M_{GZI} = diag\left\{U_1^{(z)H}, \dots, U_K^{(z)H}\right\} \qquad (3.25)$$

3.2.7. Generalized MMSE Channel Inversion

The biggest flaw of the block diagonalization and GZI comes from ignoring the noise effects on the received signal, provoking a noise enhancement thus stopping the lineal growth of the data rate with the number of users and transmit antennas. The generalized MMSE channel inversion (GMI) solves the issue by taking into consideration more than the channel matrix when creating the precoding matrix.

The GMI precoder matrix calculation starts by the calculation of (3.26) where the parameter $\alpha = \frac{N_r \sigma_\omega^2}{P_{total}}$, taking the SNR into consideration for the solution. Next we apply to it the QR decomposition as the GZI did, obtaining (3.27). As learned in the previous section $\overline{Q}_j$ composes the orthonormal base for the null space of $\overline{H}_j$ but in this case the matrix will not perfectly cancel the signal from other users because it created a residual interference. To solve the issue an interference suppression process is needed additionally.

$$\overline{H} = (H^H H + \alpha I)^{-1} H^H \qquad (3.26)$$

30

The interference suppression process is done through a combining matrix T_j applied to $\overline{Q}_j$, obtaining the received signal from (3.27). Applying the SVD decomposition to $H_j\overline{Q}_jT_j = U_j^{(m)}S_j^{(m)}V_j^{(m)^H}$ just like done in the second steps of BD or GZI we can obtain the detector matrix $M_j = U_j^{(m)^H}$ and the last part of the precoder $V_j^{(m)}$ with currently unknown values until T_j is calculated.

$$y_j = H_j\overline{Q}_jT_jx_j + H_j\sum_{k=1;k\neq j}^{K}\overline{Q}_jT_kx_k + n_j \qquad (3.27)$$

To calculate the values of T_j and consequently the rest of the precoder and decoder matrixes two options are presented, one with total power constraint and minimum interference plus noise power criterion under per user power constraint. A more detailed explanation of the process can be found at [17].

For the first option the matrix T_j is separated into a scaling parameter β and a vector $T_j = \beta \overline{T}_j$. With this separation we can solve the constraint problem of power allocation which minimizes the mean square error of the specific user with a first step where $\overline{T}_j$ is calculated as indicated in (3.28) and a second one where β is calculated as indicated in (3.29).

$$\overline{T}_j = \left(\overline{Q}_j^{\ H}\sum_{k=1}^{K}H_k^{\ H}H_k\overline{Q}_j + \alpha I_{nj}\right)^{-1}\overline{Q}_j^{\ H}H_j^{\ H}H_j\overline{Q}_j \qquad (3.28)$$

$$\beta = \sqrt{P_{total}}\left[\sum_{j=1}^{K}Trace\left(\overline{T}_j^{\ H}\overline{T}_j\right)\right]^{-\frac{1}{2}} \qquad (3.29)$$

In the second option, attractive when establishing the power allocation manually is necessary, the first step is allocating the power to each user p_j, with a constraint in total transmitted power (3.30). Afterward we calculate $T_j = p_j\overline{T}_j$ through the compute of the minimization expressed on equation (3.31).

$$Trace\left(T_j^{\ H}T_j\right) = N_jp_j^{\ 2}$$
$$constrained\ by \sum_{j=1}^{K}N_jp_j^{\ 2} \leq P_{total} \qquad (3.30)$$

$$\min_{\overline{T}_j}p_j^2\left[Trace\left(\overline{T}_j^{\ H}\overline{L}_j^H\overline{L}_j\overline{T}_j\right)\right]$$
$$Considering \quad \overline{Q}_j^{\ H}\sum_{k\neq j}H_k^{\ H}H_k\overline{Q}_j + \frac{\sigma_\omega^2}{p_j^2}I_{N_j} = \overline{L}_j^H\overline{L}_j \qquad (3.31)$$

UNIVERSITAT
POLITÈCNICA
DE VALÈNCIA

_TELECOM ESCUELA
TÉCNICA VLC SUPERIOR
DE INGENIERÍA DE
TELECOMUNICACIÓN

In both cases when the SNR is very high $\overline{T}_j$ approximates to the identity nullifying the effect of the combining matrix. After the calculation of T_j we proceed as explained before and calculate the precoding and decoding matrixes as (3.32, 3.33). With those values the sum rate of this precoder is calculated with the expression (3.34), the main difference with the previous cases is the lack of waterfilling as a solution for the power allocation, specifically in the first method it already computes the power allocation, making waterfilling unnecessary; and in the second case the solution is hard to find because each change in the power allocation changes the residual interference.

$$P_{GMI} = \left[\overline{Q}_1 T_1 V_1^{(m)}, \dots, \overline{Q}_K T_K V_K^{(m)} \right] \tag{3.32}$$

$$M_{GMI} = diag \left\{ U_1^{(m)^H}, \dots, U_K^{(m)^H} \right\} \tag{3.33}$$

$$R_{GMI} = \sum_{j=1}^{K} \sum_{i=1}^{N_j} log_2 \left(1 + \frac{\left(S_{j,i}^{(m)} \right)^2}{\sigma_\omega^2 + \sum_{k \neq j} \left\| M_{j,i} H_j P_{k_{GMI}} \right\|^2} \right) \tag{3.34}$$

3.3. Theoretical comparison

To compare the different MU-MIMO precoders analysed in this section a script comparing their performances have been generated, incorporating the precoders ZF, BD, GZI and GMI implemented with the first method of total power constraint. The scripts generate the same channel for all the precoders and then proceed to create the precoding and decoding matrixes, as explained in this section and with them calculate the obtainable data rate for each of them over the number of users in the system from one to the number necessary to occupy all the available spatial streams.

The script contains three main parametric inputs: the number of antennas in the transmitter and receiver to analyse the effect of having receivers on the network with different number of antennas; the signal to noise ratio, by adjusting either of the noise or transmitted power; and the power allocation by either take into consideration the user power or the total power in the system. Also, it additionally allows to use either a Gaussian random channel or extract the channel from the models used by the simulator.

The first point of comparison is between a 16 transmit antenna system with two antenna users in a Gaussian random channel with fixed total transmit power, as seen in figure 3-2. In it we can see firstly how all this precoders converge into the same result;
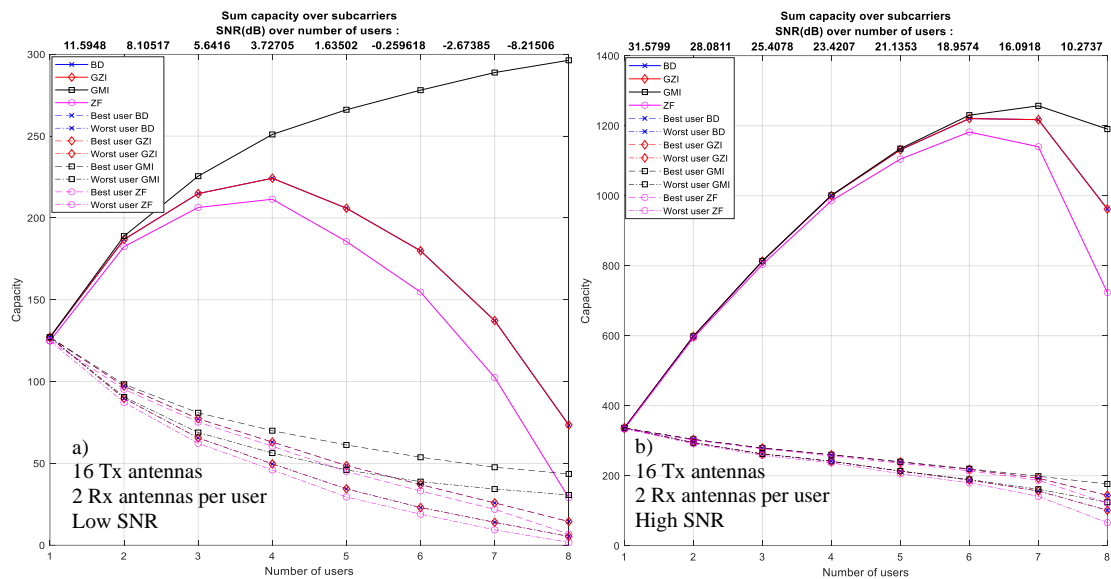
UNIVERSITAT
POLITÈCNICA
DE VALÈNCIA

TELECOM ESCUELA
TÉCNICA VLC SUPERIOR
DE INGENIERÍA DE
TELECOMUNICACIÓN

Figure 3-2 High SNR vs Low SNR comparison Gaussian channel with fixed total transmit power

explained by their structure all of them consist of a first step that cancels the multiuser interferences and an identical second step that separates each user subchannels, by removing the necessity of the first part the only remaining section of the precoders is the identical second step. Also, the identical behaviour between the BD and GZI precoders can be appreciated. Another interesting detail comes from the ZF precoder which follows closely the BD precoder with a small gap that grows with the SNR. In terms of the GMI we appreciate a clear improvement in the performance, especially in the lower SNR case where the maximum capacity keeps growing with the introduction of users despite the other precoders experimenting a steep decline after the fourth user in the network in the lower SNR case and the sixth in the high SNR scenario. The loss of capacity comes from two main factors, the first one is the increase of interferences created by the introduction of users into the system and the second one comes from the dilution of power when it is shared between a higher number of users moreover, we can see how the difference between the best and worst users is considerably higher in the low SNR case. Although the general behaviour of the system improves with the extra amount of total transmitted

power we can appreciate the same tendencies as before but because the user power remains constant the individual performance manages to grow until six and seven users for the low SNR case and high SNR case respectively.

As the next point of comparison, the figure 3-3 contains the comparison between a high SNR system with 16 transmit antennas, two antennas per receiver, random Gaussian channel and fixed user power. The first remark is see how the SNR dropped from one user to eight approximately 11dB, in comparison to the figure 3-2 that maintain the same parameters but fixed total transmit power the drops amount to 20dB. Comparing them we can appreciate how the fist case keeps the user power constant while dropping 11dB due to the interference from the other users, on the other hand the previous example dropped 20dB with a combination of interferences and power dilution between users.
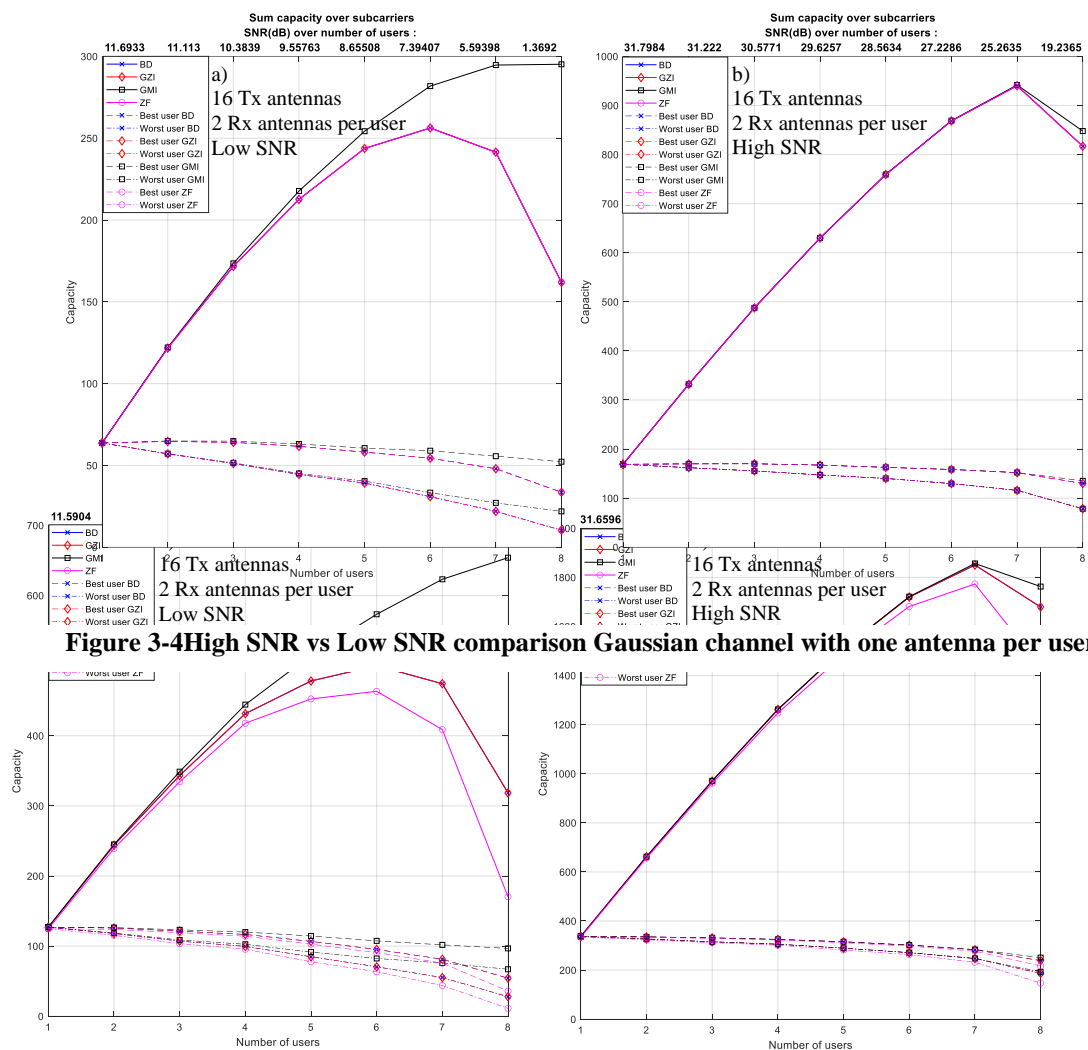

Figure 3-4High SNR vs Low SNR comparison Gaussian channel with one antenna per user

Figure 3-3 High SNR vs Low SNR comparison Gaussian channel with fixed user transmit power

The next simulation scenario offers us 8 antennas in the transmitter with one antenna per user in a Gaussian channel and fixed user power, as seen in figure 3-4, keep a consistent behaviour with the previous cases but with two main differences. The first one is the overlap of the ZF and BD precoders which is expected because as the theory states the ZF precoder is not appropriate for multiuser communications with users using more than one antenna. The second one is a closer performance between the GZI and GMI or BD precoders, especially in the high SNR scenario where they practically overlap until the final scenario with eight users.

The final scenario to analyse is the non-Gaussian channel, specifically in this case we are using a channel model E from the models used by the simulator that will be used to perform the simulations. The system consists of a 8 antenna transmitter and 2 antenna receivers and its behaviour is reflected in the figure 3-5. In the first part the most relevant changes from the Gaussian channel is the difference from the ZF precoder and the rest at the one user point. In the second part we can see rapid changes in the performance following the channel response with a gap between the precoders, seeing that not only the GMI offers a better performance but also a less variant performance over the spectrum.
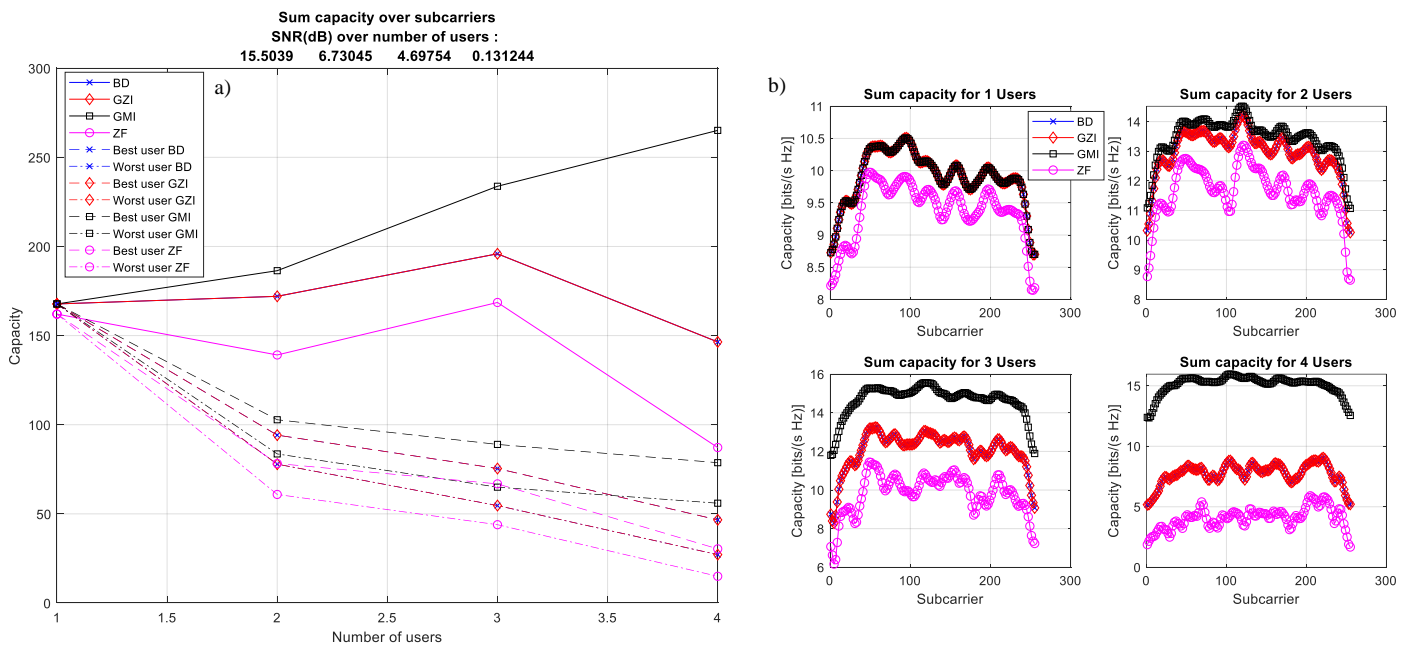

Figure 3-5 non-Gaussian channel precoder performance. a) Depending on number of users | b) frequency response

4. Simulator

The simulator that will be used for this thesis is the FSIM, a proprietary simulator implemented in Matlab by the company Maxlinear where the project was realized during an internship. FSIM is a Wi-Fi simulator which includes all the link level characteristics, as the block diagram from figure 4-1 shows.
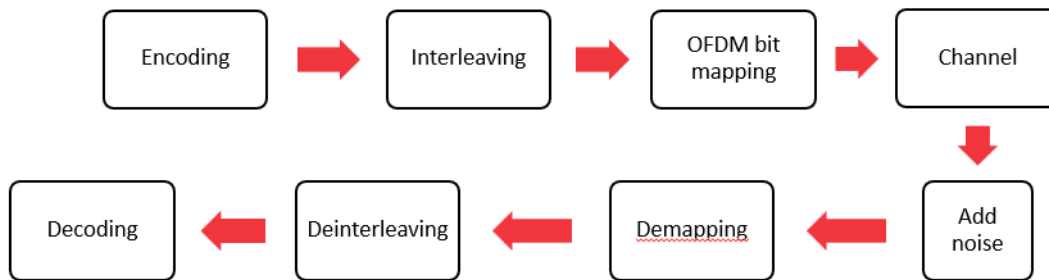

Figure 4-1 FSIM simulator system block diagram

The simulator encapsulates the whole transmission from the generation of bits to its transmission and posterior reception just like a real Wi-Fi system would. It has a long list of parameters letting the user configure all the steps of the process with all the options given by the 802.11 standard.

The biggest limitation of the FSIM is that it only simulates the data subcarriers removing the pilot subcarriers from the simulation and it doesn't incorporate the packet preambles limiting in multiple aspects but primarily in terms of channel sounding. For the channel modelling the simulator uses the channels models created by the Task Group N for the release of the 802.11n standard that have been updated with each successive release.

The simulator has an extensive parametrization, aside from the basic ones like the channel bandwidth or MCS that are expected we can spotlight some of the most relevant for this project. In the detector options we have used mainly four of them, the ZF detector and the MMSE detectors as explained in the theoretical part and two versions of the sphere decoder [18] the maximum likelihood (ML) detector and an approximation to the ML detector. In terms of precoders for the SU-MIMO simulations we can opt to not use them or utilize the SVD precoder as explained in the theoretical part. On the other hand, the precoders for the MU-MIMO offer three options: the block diagonalization, the ZF precoder as explained in the theory and the MMSE utilizing the uplink-downlink duality [19].

The simulator incorporated two main methods of simulating, firstly the direct simulation mode where the simulator would compute the full transmission under the given parameters to calculate the BER at the receiver. The second method was an MCS search where the simulator would try each MCS for every step on the process until it finds the highest one that respects the BER condition.

4.1. Channel Models

The channel model used for the simulations are given by the Wi-Fi standardization teams. Starting with 802.11n the Wi-Fi standard introduced MIMO capabilities into the system thus a channel model which allowed the correct analysis of the channel effect over the communication. To fulfil this necessity the Task Group N (TGn) created a set of channel models [20] applicable to indoor MIMO systems. With the releases of new versions of the standard the different task groups have updated the models [21-23] introducing new elements and updating existing ones to keep the models up to date with the standard features. As the describing document the models were based on the previous SISO models proposed by Mebdo et al. [24-25] and the multiple antenna models were based on the ones developed by Saleh and Valenzuela [26].

The channel models are based on taps, to represent the power delay profile of the received signal. To model the different times of arrival and directions of the different multipath elements created in the environment the models group them into clusters, under the assumption that the sources of scatter are normally grouped creating multiple components with similar special characteristics. For each one of the models proposed several clusters, between two and six was given and proves to behave similar to experimental results and ray tracing methods. The tap power for each cluster was given to ensure that the sum of overlapping taps correspond to the original tap delay profiles. The rest of the relevant parameters in the models, angular spread (AS), angle of arrival (AoA) and angle of departure (AoD); were assigned to each tap and cluster with values that agree with the experimental values obtained in different reports. The full list of values for the model can be found on the Annex C of [20].

There are six channel models, three from the original SISO models and three additional ones, named alphabetically starting with A for the smaller environments. The model A is an optional irreal model not meant to compare system performances; it is a

flat fading model with 0ns of rms delay spread, it only consists of one tap. The model B is meant to represent a residential indoor scenario with small rooms; it uses two clusters with five and seven taps respectively and a delay spread of 15ns. The model C represents small offices or big residential scenarios; it consists of two clusters with ten and eight taps and a delay spread of 30ns. The model D represent typical office scenarios with big rooms like cube farms or classrooms in the academia environment; to model it the model assigns a delay spread of 50ns and three clusters of 16, 7 and 4 taps respectively. The model E represents large rooms like a warehouse; for it uses four clusters with 15, 12, 7 and 4 taps with a delay spread of 100ns. The last model F model large indoor spaces like an airport that can be considered pseudo-outdoor spaces; in this scenario six clusters are used with 15, 12, 7, 3, 2 and 2 taps respectively with a delay spread of 150ns. A table resuming all the parameters described previously can be found in Table 2.

Table 2: Channel Model Parameters

Model	Delay spread RMS (ns)	Number of Clusters	Taps/Cluster	Rician K-factor (dB)
A	0	1	1	0
B	15	2	5, 7	0
C	30	2	10, 8	0
D	50	3	16, 7, 4	3
E	100	4	15, 12, 7, 4	6
F	150	6	15, 12, 7, 3, 2, 2	6

The Rician K-factor indicates the ratio between the direct path and the scattered paths, with a high value the LOS path predominates meanwhile with a value of zero the direct path disappears. The Table 1 gives the specified K-factor for each model, in the case it represents a LOS scenario, in the NLOS case it will be valued $-\infty$dB indicating it has no impact. The base model tap values don´t take the LOS case into consideration, in order to include their influence in the channel the model indicates that we will add extra power to the first tap according to the K-factor, assuming that the rest of the taps have a factor of $-\infty$dB.

4.1.1. Pathloss model

The pathloss model is divided in two parts, an indoor and an outdoor model. Initially the pathloss only incorporated a two-ray model to model the indoor loses and later, in the revision for 802.11ax, it was expanded adding the losses created traversing walls and floors and an outdoors model based on the ITU-R model developed by the 3GPP, it has two different models, the urban micro (UMi) and the urban macro (UMa), both of them can be used for the simulation of Wi-Fi systems. In UMi both antennas are located under the buildings height and is the principal model, on the other hand UMa situates the AP outdoors with a location above the buildings and serves a complementary role to Umi.

The two-ray model considers the losses as free space losses until a breakpoint distance where the slope grows. The equations (4.1, 4.2) include the expressions utilized, where L represents the losses, L_{FS} the free space losses, d the separation distance in meters and d_{BP} the breakpoint distance in meters. The breakpoint distances are set by the models with a value of 5 meters for the first three models and values of 10, 20 and 30 meters for the models D, E and F respectively. Also, the model incorporates the values for the standard deviation of the shadow fading, with a value of 3dB for the first slope in all the models and for the second slope a value of 4 for the first two models, 5 for the middle two models and a value of 6 for the last two models.

$$L(d) = L_{FS}(d) \quad d \le d_{BP} \tag{4.1}$$

$$L(d) = L_{FS}(d_{BP}) + 35log_{10}\left(\frac{d}{d_{BP}}\right) \tag{4.2}$$

To take into consideration the losses created when traversing walls and floors, we calculate each type of the loses flowing the equations (4.3, 4.4) and finally add that extra loses to the total. In these equations L_{wall} indicates the losses generated at the walls, L_{floor} the losses generated traversing floors, the n the number of floors, m the number of walls and L_{iw} the losses per wall fixed to a value between 5dB and 7dB.

$$L_{floor} = 18.3 \, n^{\left(\frac{n+2}{n+1} - 0.46\right)} \tag{4.3}$$

$$L_{wall} = m \cdot L_{wall} \tag{4.4}$$

The outdoor channel model is separated in two different models, LOS and NLOS conditions; additionally exist an outdoor to indoor model. In the LOS scenario similarly to the indoor channel model has two different formulas, one until a breakpoint and a different one afterwards but, in this case instead of having fixed breakpoint distances for each model it follows the equation on (4.5), depending on the AP antenna height in meters h_{AP}, the antenna height in meters of the station h_{STA}, the carrier frequency in GHz f_c and the speed of light c in m/s. The model proposes the antenna heights of both the AP and STA as 10m and 1.5m respectively. The models utilized on the outdoor (4.6, 4.7) scenarios require a minimum distance of 10m and have a maximum distance of 5000m. The LOS scenario has a shadow fading standard deviation of 3dB.

$$d_{BP} = \frac{4(h_{AP}-1)(h_{STA}-1)f_c \cdot 10^9}{c} \tag{4.5}$$

$$L_{outdoor-LOS}(d) = 22\,log_{10}(d) + 28 + 20\,log_{10}(f_c) \quad if\ 10m \leq d < d_{BP} \tag{4.6}$$

$$L_{outdoor-LOS}(d) = 40\,log_{10}(d) + 7.8 - 18\,log_{10}(h_{AP} - 1) -$$
$$18\,log_{10}(h_{STA} - 1) + 20\,log_{10}(f_c) \quad if\ d_{BP} \leq d < 5000m \tag{4.7}$$

In the NLOS scenario the model follows the formula from equation (4.8) while the separation is higher than 10m buy lower than 2000m. The outdoor to indoor model follows the equation (4.9) is used, with d_{in} and d_{out} representing the indoor and outdoor distances respectively. The shadow fading standard deviation is of 4dB for NLOS and 7dB for outdoor to indoor.

$$L_{outdoor-NLOS}(d) = 36.7\,log_{10}(d) + 22.7 + 26\,log_{10}(f_c) \tag{4.8}$$

$$L_{outdoor-to-indoor} = L_{outdoor-NLOS}(d_{out} + d_{in}) + 20 + 0.5d_{in} \tag{4.9}$$

4.1.2. MIMO Channel Matrix

The model utilizes the transmit matrixes to create the MIMO channel matrix for each tap in each time instance. The matrix can be separated in a fixed part, corresponding to the line of sight (LOS) portion and a variable component representing the non-line of sight (NLOS) portion. In the equation (4.10) the expression of the channel matrix is represented, with P signifying the sum of all the taps power, H_F represents the fixed part

UNIVERSITAT
POLITÈCNICA
DE VALÈNCIA

_TELECOM ESCUELA
TÉCNICA VLC SUPERIOR
DE INGENIERÍA DE
TELECOMUNICACIÓN

of the matrix, H_v representing the variable part of the matrix, K representing the Rician K-factor.

$$H = \sqrt{P}\left(\sqrt{\frac{K}{K+1}}H_F + \sqrt{\frac{1}{K+1}}H_v\right) \qquad (4.10)$$

Assuming that each tap consists of a number of individual rays we can assume that the variable matrix is composed of correlated, zero mean, unit variance Gaussian random variables. Using as example a two-antenna system the MIMO matrix can be divided as equation (4.11) indicates, the X_{ij} represent the correlated Gaussian random variables from the H_v matrix; similarly in equation (4.12) we have the expression for H_F, where ϕ_{ij} represent the phase of the matrix element between the i-th receive antenna and the j-th transmit antenna.

$$H_v = \begin{bmatrix} X_{11} & X_{12} \\ X_{21} & X_{22} \end{bmatrix} \qquad (4.11)$$

$$H_F = \begin{bmatrix} e^{j\phi_{11}} & e^{j\phi_{12}} \\ e^{j\phi_{21}} & e^{j\phi_{22}} \end{bmatrix} \qquad (4.12)$$

The variable matrix correlation elements from the matrix X the expression from (2.17) is used, which utilizes the receive and transmit correlation matrixes, R_{rx} and R_{tx} respectively. The matrix H_{iid} is formed with independent, zero mean, unit variance, complex Gaussian random elements.

$$[X] = [R_{rx}]^{\frac{1}{2}}[H_{iid}]\left([R_{tx}]^{\frac{1}{2}}\right)^T \qquad (4.13)$$

4.1.3. Adaptation to new environments

The original models from the TGn had a maximum bandwidth of 40MHz that became obsolete with the introduction of higher bandwidth channels in 802.11ac and 802.11be. To adapt the model the TGac introduced a systemic method to increase the channel bandwidth reducing the tap spacing.

The first step of the process is obtaining the expansion factor k as the ratio between the new sampling rate and 100MHz ($new\ sampling\ rate = k \cdot 100MHz$). The next step consists in introducing k-1 new taps after each existing tap, spacing them 10/k ns apart, the first of them is situated 10/k ns after the primary one. The new tap power are assigned by the linear interpolation between the two basic contiguous taps. No taps will be

allocated after the last original tap. This interpolation will result in independent channel tap realizations obtaining a fundamentally different channel that the base model.

The base model assigns a closed value to the AoA and AoD of each cluster but in scenarios where multiple users are sharing the channel, for example MU-MIMO, it represents a limiting factor. To enable a different position and orientation to each user in the simulations the model the specification indicates that a random offset is added to each user AoA and AoD. To process these values correctly the model indicates the correct randomizing procedure and seeds needed.

5. Simulation results

The simulation done in this project can be separated in two, first the single user MIMO and secondly the multiuser MIMO simulations. In the first ones the focus was studying the effect over the communication of the principal parameters like the usage of beamforming or the decoder option. In the second group, the MU-MIMO simulations the main focus was on one hand the comparison between the available precoders and on the other hand compare the performance of the multiuser scheme over the single user, answering the question when its better to user MU-MIMO over sequential SU-MIMO communications.

5.1. SU-MIMO simulations

. The basic configuration for the simulations was a 20MHz bandwidth, 4 antennas in both the transmitter and receiver, two different spatial streams, channel model B, SVD beamforming, LDPC encoding, MCS 8 and ZF decoder. Each simulation deviates from the configuration in the aspects it tries to analyse keeping the rest constant.

The first simulation performed in this project was a comparison of the different decoders on the same channel configuration. The result can be seen on figure 5-1 where we can appreciate a gap of approximately 0.5dB between the two implementations of the sphere decoder and the linear decoders. The general behaviour is a curve that lowers the BER as the SNR grows; at high SNR values the curves become messy due to the simulation limitations, the number of simulated bits needed to obtain a high enough
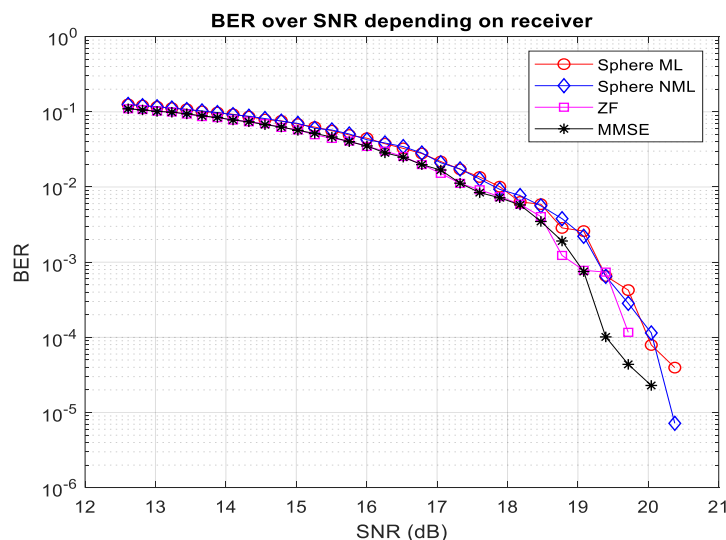

Figure 5-1 BER over SNR curve for different decoders

UNIVERSITAT
POLITÈCNICA
DE VALÈNCIA

TELECOM ESCUELA
TÉCNICA VLC SUPERIOR
DE INGENIERÍA DE
TELECOMUNICACIÓN

number of errors to keep the curve pattern was too big for the allowed resources at the time.
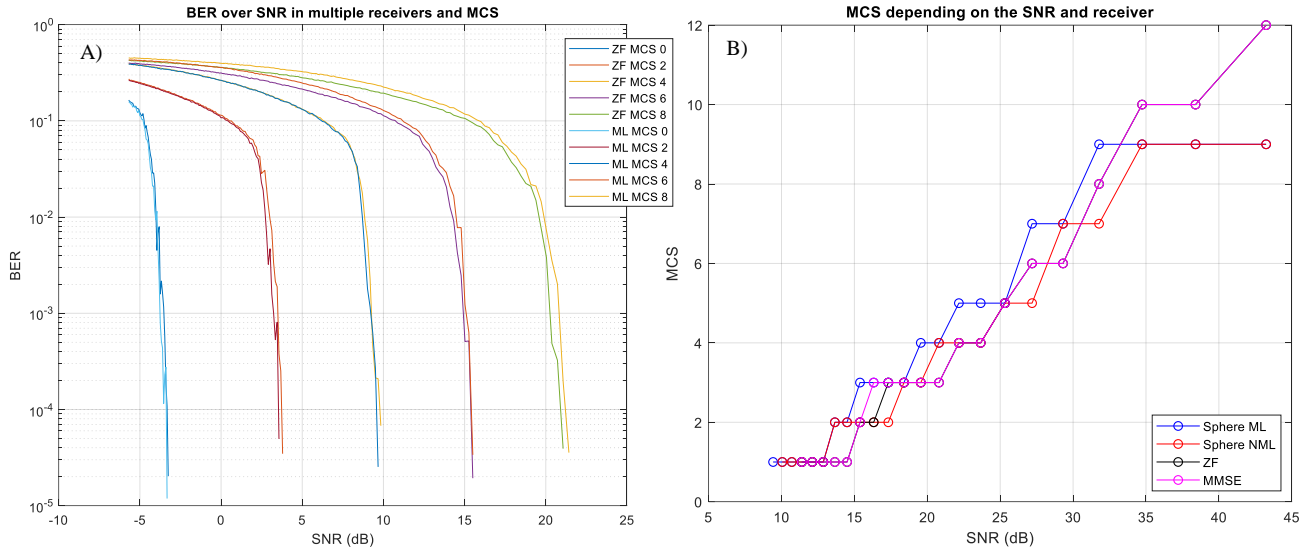

Figure 5-2 MCS comparison. A) Different MCS BERvsSNR B) Best MCS at each SNR

The second simulation, as seen in Figure 5-2 compares different MCS, the first graph compares the performance of various MCS over SNR with two different decoders showing that the lower MCS in a steeper curve in comparison to the higher MCS values. Also it shows that the performance difference between the ZF and ML precoders is higher with higher MCS and is almost irrelevant in the lower at lower MCS values. The second graph is the realization of the MCS search, obtaining the best MCS for each step with the
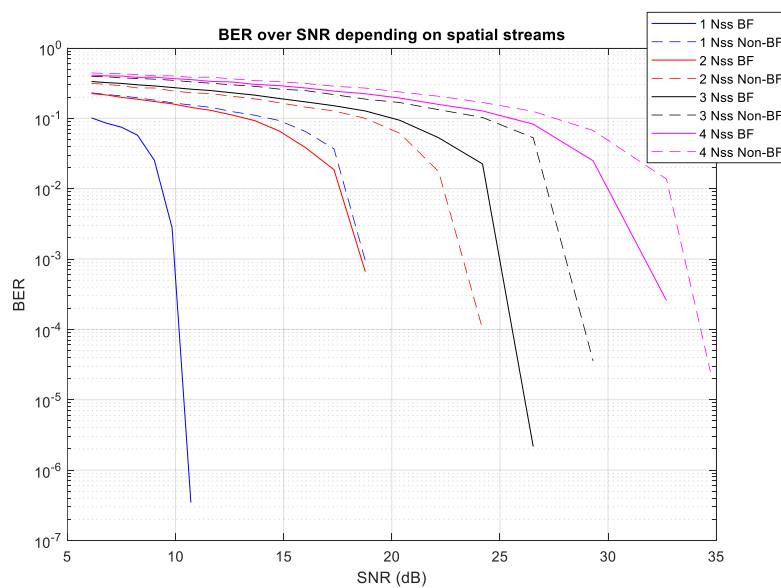

Figure 5-3 Performance analysis depending on the precoder at multiple number of spatial streams

different decoders. We can see how the ML sphere decoder offers overall a better performance, up to the MCS 9 where the simulator limits the sphere decoders due to complexity, and the almost complete overlap between the MMSE and ZF decoders.

The next simulation evaluates the performance of the beamforming in figure 5-3, comparing using the SVD precoder over not using it depending on the number of spatial streams. The first take away is the improvement of the BER with a lower number of spatial streams that comes from the fact that the MIMO systems use the best spatial streams first so each one added will have a worse performance than the last. The second notable behavior is how the improvement from implementing beamforming is higher in the systems with less spatial streams utilized. This phenomenon coincides with the tradeoff between capacity and reliability, selecting more spatial streams, thus capacity, lowers the reliability and vice versa.

The last simulation for the SU-MIMO case is the data rate obtainable over the SNR received, figures 5-4 and 5-5. For this scenario we have analyzed the performance of the system under various maximum data rates by varying the MCS and the number of spatial streams and we have selected all the cases that offered a BER higher than a threshold of $BER \leq 10^{-5}$. In the figure 5-4 we see the case for a channel model B and we can appreciate the different curves crossing between them, indicating that with less than 5 dB SNR we should use one spatial stream, until 15dB the optimal solution is using
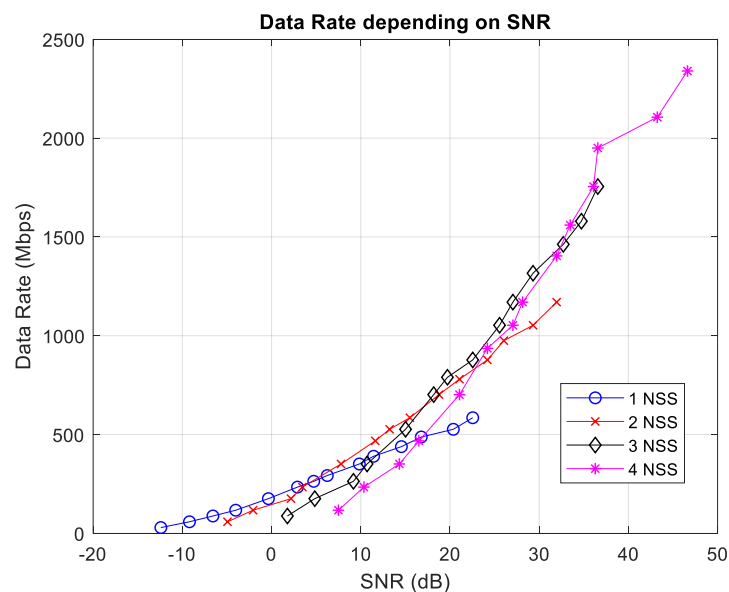

Figure 5-4 Maximum obtainable data rate over SNR in channel model B

two spatial streams and four spatial streams should be used in systems with more than 30 dB SNR. The rest of the channel models in figure 5-5 offer a similar performance with variations over the thresholds.
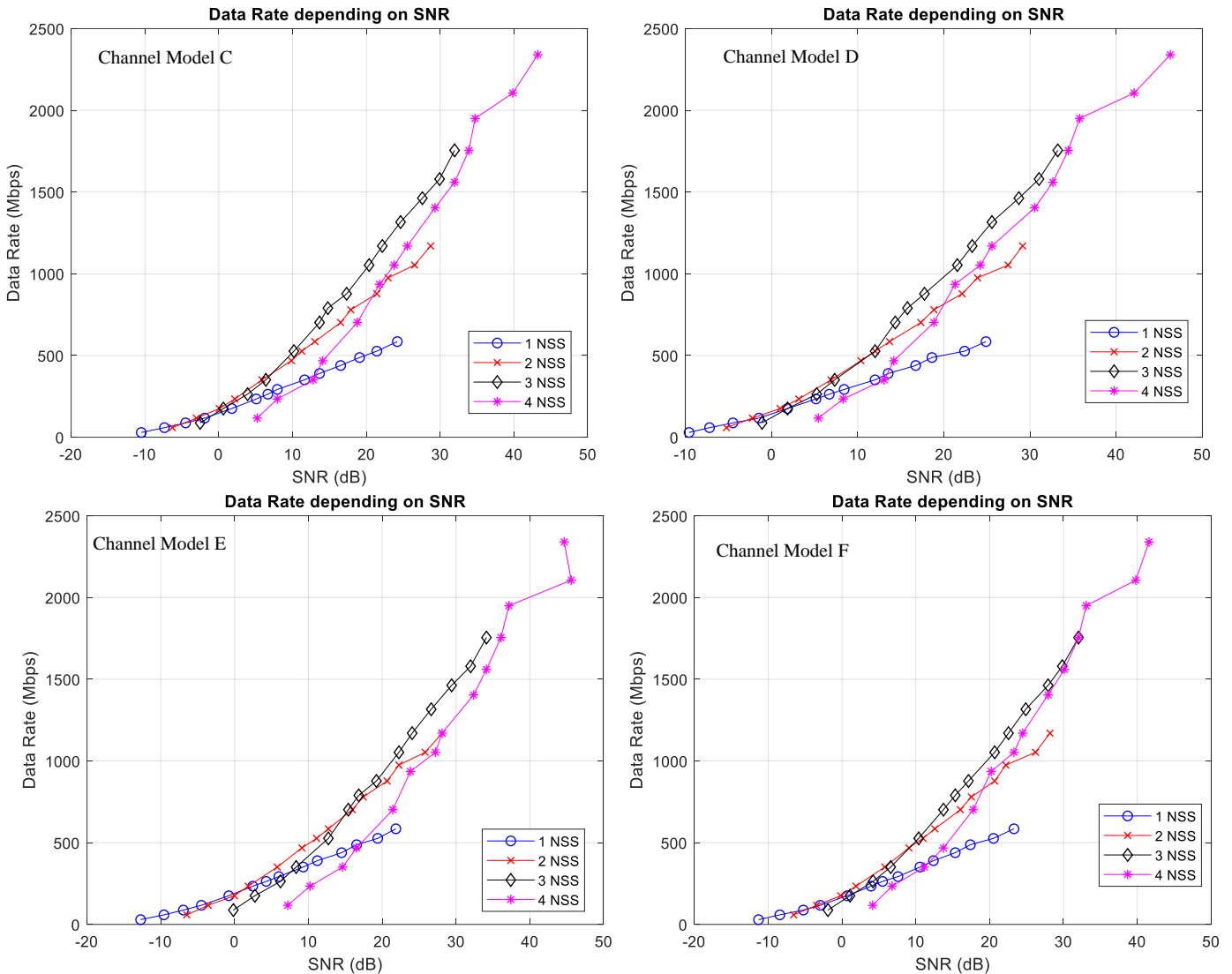

Figure 5-5Maximum obtainable data rate over SNR in channel models C, D, E and F

5.2. MU-MIMO simulations

For the MU-MIMO scenario only two simulations have been carried out. First, the comparison of precoders and then a capacity calculation over the number of users involved in the communication, comparing the use case of multiuser communication with communicating with each user sequentially with a higher data rate.
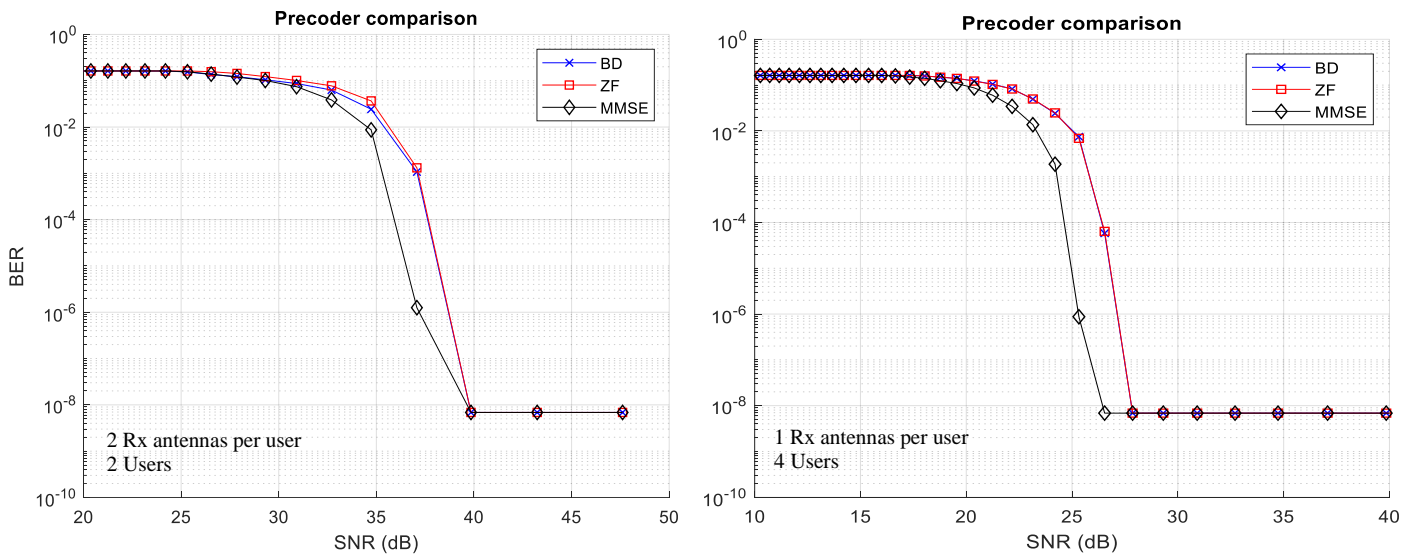
Figure 5-6 Precoder comparison in MU-MIMO

The configuration for the precoder comparison is based on a channel model B with a MCS of 8 and 4 antennas at the transmitter. The number of antennas was selected because it was the number of antennas the company's current device was limited to that amount. For the user we have selected two scenarios, a first one with two antennas per user with a maximum of two users and user with one single antenna enabling the communication up to four simultaneous users. The results for these two scenarios are found on figure 5-6 where the average result between the users in the system is displayed. Like the theoretical calculations the BD and ZF precoders offer the exact same performance in the case with one antenna per user and with multiple antennas per receiver the BD outperforms slightly the ZF precoder. On the other hand, the MMSE precoder implemented through the uplink-downlink duality offer a clear advantage to the other two precoders in both cases, offering around a 2dB improvement over the others.

The last simulation intends to express the channel capacity depending on the number of users and the SNR, the results can be seen at the figures 5-7 and 5-8 with one and two antenna receivers respectively. In these simulations, like in the similar SU-MIMO scenario, we have calculated at each SNR value the performance of the different MCS and selected the one where all the users accomplished $BER \leq 10^{-5}$. For this scenario we have used the BD precoder.

In the figures we have two graphs, on one hand we compare the maximum MCS attainable for each user depending on the number of users, on the other hand the MCS

UNIVERSITAT
POLITÈCNICA
DE VALÈNCIA

TELECOM ESCUELA
TÉCNICA VLC SUPERIOR
DE INGENIERÍA DE
TELECOMUNICACIÓN

obtained in the first one is translated into an average user capacity value taking onto consideration both the MCS and the number of streams available. In the first one we can see how each user added to the system has a lower performance than the already existing ones; this is caused by two factors, firstly each user in the network will increase the multiuser interferences introduces in the system that may not be perfectly decoupled in some precoding techniques and secondly each spatial stream available will have a worse channel response than the ones already being used. With these conditions taken into consideration we can see how the capacity graph shows that depending on the SNR the usage of MU-MIMO may be suboptimal in comparison to multiple consecutive single user communication from the capacity point of view. Moreover, in the case with multiple steps in the introduction of users we will see as optimal the progressive introduction of them depending on the SNR.
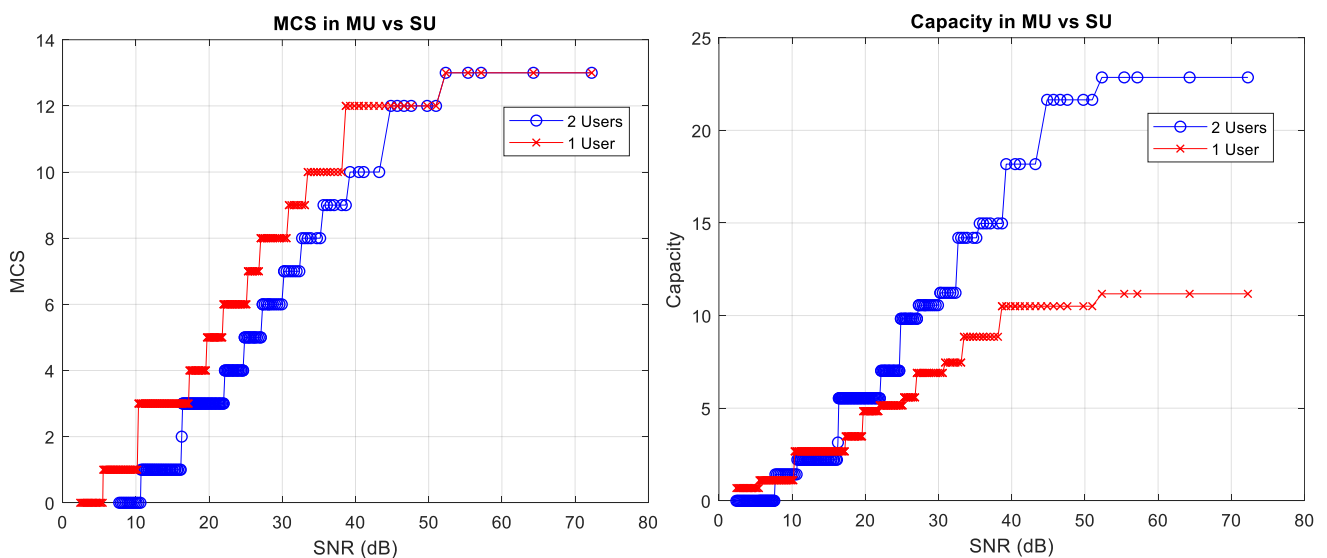
Figure 5-7 Capacity simulation in a MU-MIMO system with 2 antennas at each receiver.
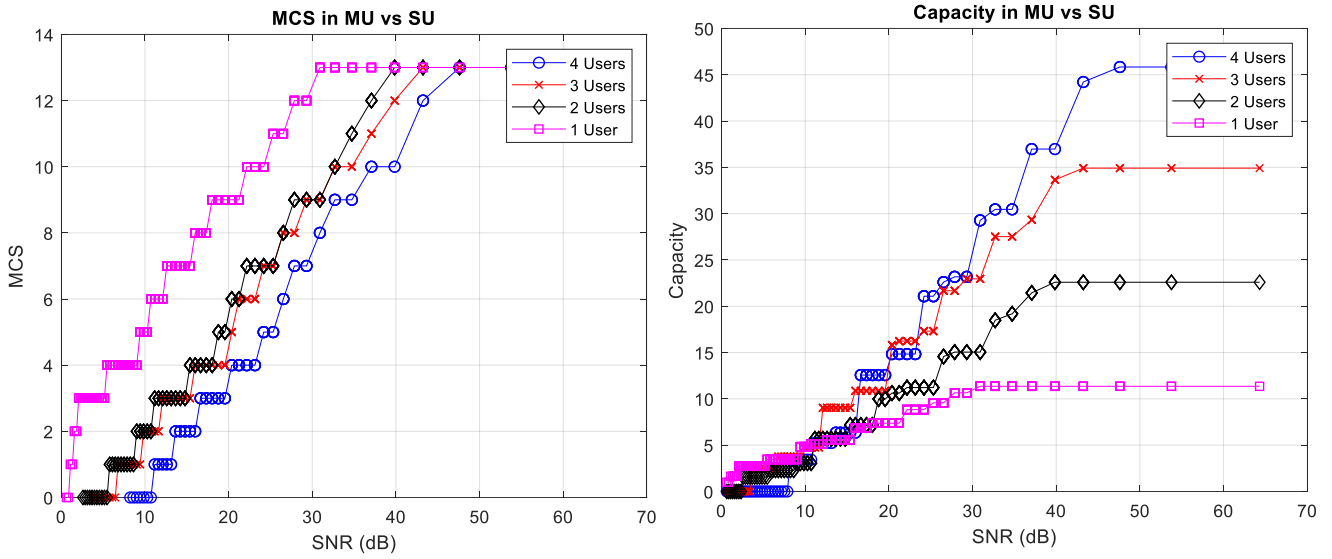**a) expressed in MCS b) expressed in capacity**

Figure 5-8 Capacity simulation in a MU-MIMO system with 1 antenna at each receiver.
a) expressed in MCS b) expressed in capacity

6. Conclusions and Future Work

6.1. Conclusion

In this work we realized a study of the Wi-Fi standards focusing on the PHY layer; the study covered from the earlier versions of the standard through its evolution with the incorporation of nowadays essential elements of the standard like OFDM or MIMO. The study focused on the link level simulation, reviewing from the base technologies enabling the Wi-Fi systems specially on the multiuser communications both OFDMA with the frequency multiplexing and MU-MIMO with the spatial multiplexing.

For the simulation we reviewed the proprietary simulator facilitated by the company where the project was realized during an internship. With it we simulated both the single user MIMO communications and MU-MIMO communications.

In the simulations we have shown the advantages of using these technologies, from the spatial redundancy improving the reliability of the communications to the data rate increase from the parallel data streams in the single user communications to the benefits of using MU-MIMO in good channel conditions to further increase the total capacity of the system where the central node has more resources than the user devices. We can ensure that the strengths of MU-MIMO align with the necessities of Wi-Fi and the benefits that it provides.

The SU-MIMO simulations show how the more complex detectors offer a performance increase of 0.5 dB respectively of the simpler ones in terms of raw BER. When comparing a capacity metric, we can see how they can enable the use of a higher MCS thus offering a higher throughput. However, this precoders have a higher complexity that can be the limiting factor for devices with low resources. When analizing the spatial diversity we can appreciate how the usage of multiple parallel data streams can only be done with higher SNR and at lower SNR the usage of less data streams offer overall a better performance.

In the MU-MIMO simulations we see how the uplink-downlink duality based MMSE precoder offer a 1 dB improvement over the BD or ZF precoders. These two offer the same response with one antenna receivers and a small performance increase for the BD when the receiver incorporates multiple antennas. In terms of capacity we see how at

low SNR values is more beneficial to use SU-MIMO communications and as the SNR increases increase the number of users.

6.2. Future work

The future lines of work in this project consist mainly in two options, firstly we can add more simulations options especially the uplink communication that was originally planned but due to times constraints it was unable to finish. Other options come from expanding the simulated parameters, like the incorporation of the theoretically explained precoders GZI and GMI. Also, the incorporation of the new requirements for the 802.11be standard is a logical extension of the work done.

The second line of improvement comes from improving the simulator with the main feature being the implementation of the pilot subcarrier and packet preambles to simulate more accurately the real conditions, having into consideration the channel estimation and the communication of the communication parameters through the preambles.

7. REFERENCES

[1]   "IEEE Standard for Information Technology--Telecommunications and Information Exchange between Systems - Local and Metropolitan Area Networks--Specific Requirements - Part 11: Wireless LAN Medium Access Control (MAC) and Physical Layer (PHY) Specifications," in IEEE Std 802.11-2020 (Revision of IEEE Std 802.11-2016) , vol., no., pp.1-4379, 26 Feb. 2021, doi: 10.1109/IEEESTD.2021.9363693.

[2]   E. Perahia and R. Stacey, Next generation wireless LANs : 802.11n, 802.11ac, and Wi-Fi direct / [electronic resource], Second edition. Cambridge: Cambridge University Press, 2013.

[3]   E. Khorov, A. Kiryanov, A. Lyakhov and G. Bianchi, "A Tutorial on IEEE 802.11ax High Efficiency WLANs," in IEEE Communications Surveys & Tutorials, vol. 21, no. 1, pp. 197-216, Firstquarter 2019, doi: 10.1109/COMST.2018.2871099.

[4]   "IEEE Standard for Information Technology--Telecommunications and Information Exchange between Systems Local and Metropolitan Area Networks--Specific Requirements Part 11: Wireless LAN Medium Access Control (MAC) and Physical Layer (PHY) Specifications Amendment 1: Enhancements for High-Efficiency WLAN," in IEEE Std 802.11ax-2021 (Amendment to IEEE Std 802.11-2020) , vol., no., pp.1-767, 19 May 2021, doi: 10.1109/IEEESTD.2021.9442429.

[5]   S. Muhammad, J. Zhao and H. H. Refai, "An Empirical Analysis of IEEE 802.11 ax," 2020 International Conference on Communications, Signal Processing, and their Applications (ICCSPA), 2021, pp. 1-6, doi: 10.1109/ICCSPA49915.2021.9385748.

[6]   https://www.rfglobalnet.com/doc/wi-fi-s-ofdma-challenges-make-verification-crucial-0001

[7]   E. Khorov, I. Levitsky and I. F. Akyildiz, "Current Status and Directions of IEEE 802.11be, the Future Wi-Fi 7," in IEEE Access, vol. 8, pp. 88664-88688, 2020, doi: 10.1109/ACCESS.2020.2993448.

[8]   Garcia-Rodriguez, Adrian & Lopez-Perez, David & Galati Giordano, Lorenzo & Geraci, Giovanni. (2021). IEEE 802.11be: Wi-Fi 7 Strikes Back. IEEE Communications Magazine. 59. 102-108. 10.1109/MCOM.001.2000711.

[9]   C. Deng et al., "IEEE 802.11be Wi-Fi 7: New Challenges and Opportunities," in IEEE Communications Surveys & Tutorials, vol. 22, no. 4, pp. 2136-2166, Fourthquarter 2020, doi: 10.1109/COMST.2020.3012715.

[10]   D. Lopez-Perez, A. Garcia-Rodriguez, L. Galati-Giordano, M. Kasslin and K. Doppler, "IEEE 802.11be Extremely High Throughput: The Next Generation of Wi-Fi Technology Beyond 802.11ax," in IEEE Communications Magazine, vol. 57, no. 9, pp. 113-119, September 2019, doi: 10.1109/MCOM.001.1900338.

[11]   R. Penrose, "A generalized inverse for matrices," Mathematical Proceedings of the Cambridge Philosophical Society, vol. 51, no. 3, pp. 406–413, 1955.

[12]   A. Farzamnia, E. Moung, N. W. Hlaing, L. E. Kong, M. K. Haldar and L. C. Fan, "Analysis of MIMO System through Zero Forcing and Minimum Mean Square Error Detection Scheme," 2018 9th IEEE Control and System Graduate Research Colloquium (ICSGRC), 2018, pp. 172-176, doi: 10.1109/ICSGRC.2018.8657515.

[13]   G. Lebrun, J. Gao and M. Faulkner, "MIMO transmission over a time-varying channel using SVD," in IEEE Transactions on Wireless Communications, vol. 4, no. 2, pp. 757-764, March 2005, doi: 10.1109/TWC.2004.840199.

[14]   C. B. Peel, B. M. Hochwald and A. L. Swindlehurst, "A vector-perturbation technique for near-capacity multiantenna multiuser communication-part I: channel inversion and regularization," in IEEE Transactions on Communications, vol. 53, no. 1, pp. 195-202, Jan. 2005, doi: 10.1109/TCOMM.2004.840638.

[15]   Q. H. Spencer, A. L. Swindlehurst and M. Haardt, "Zero-forcing methods for downlink spatial multiplexing in multiuser MIMO channels," in IEEE Transactions on Signal Processing, vol. 52, no. 2, pp. 461-471, Feb. 2004, doi: 10.1109/TSP.2003.821107.

[16]   D. P. Palomar and J. R. Fonollosa, "Practical algorithms for a family of waterfilling solutions," in IEEE Transactions on Signal Processing, vol. 53, no. 2, pp. 686-695, Feb. 2005, doi: 10.1109/TSP.2004.840816.

[17]   H. Sung, S. -. Lee and I. Lee, "Generalized Channel Inversion Methods for Multiuser MIMO Systems," in IEEE Transactions on Communications, vol. 57, no. 11, pp. 3489-3499, Nov. 2009, doi: 10.1109/TCOMM.2009.11.070404.

[18]   Mong Suan Yee, "Max-log-MAP sphere decoder," Proceedings. (ICASSP '05). IEEE International Conference on Acoustics, Speech, and Signal Processing, 2005., 2005, pp. iii/1013-iii/1016 Vol. 3, doi: 10.1109/ICASSP.2005.1415884.

[19]   Strobel, Rainer. Channel Modeling and Physical Layer Optimization in Copper Line Networks. Springer International Publishing, 2019, pp. 65-70.

[20]   Erceg, V., L. Schumacher, P. Kyritsi, et al. TGn Channel Models. Version 4. IEEE 802.11-03/940r4, May 2004.

[21]   Breit, G., H. Sampath, S. Vermani, et al. TGac Channel Model Addendum. Version 12. IEEE 802.11-09/0308r12, March 2010..

[22]   Jianhan, L., Ron, P. et al. TGax Channel Model. IEEE 802.11-14/0882r4, September 2014.

[23]   J. Liu, "IEEE 802.11be Channel Model Document," IEEE 802.11-19/0719r1, May 2019.

[24]   J. Medbo and J-E. Berg, "Measured radiowave propagation characteristics at 5 GHz for typical HIPERLAN/2 scenarios," ETSI/BRAN document no. 3ERI084A.

[25]   J. Medbo and P. Schramm, "Channel models for HIPERLAN/2," ETSI/BRAN document no. 3ERI085B

[26]   A.A.M. Saleh and R.A. Valenzuela, "A statistical model for indoor multipath propagation," IEEE J. Select. Areas Commun., vol. 5, 1987, pp. 128-137.

8. ANNEX I: Scripts for theoretical comparison

```matlab
%% Theoretical comparison
for model  = ['B']

Nt = 16;  % Max 8 for channels from model
Nr = 4;    % Nu*Nr max Nt
Nu = 1:Nt/Nr;
Fixed_User_Power = 1; % 1: Each user power constant, variable total tx power
                      % 0: Each user power variable, constant total tx power
channel = 1; % 1: Gausian random channel |  0: from channel models
Nrep = 50;  % Max 50 if channel from models
sb = 1:16:256; % Subcarriers in the model, max 256
sigma2 =1;
Ptot = 100;
los = 1; % 1 = LOS; 0 = NLOS;
freq = '5'; % '5' or '2.4'
path = 'C:\Users\abarreda\Documents\MATLAB\MimoChannels\400Mhz_8x8';


randn('seed',sum(clock));
seed_rng = floor(rand*40);

for sc = sb
    for i = Nu
        for j = 1:Nrep
            if Fixed_User_Power
                Pt = Ptot*i;
            else
                Pt = Ptot;
            end
            k =j;
            [auxBD, snrBD{i,j,sc}]   = BD(Nr,Nu(i),Nt,Pt,sigma2,
(i+j)+seed_rng, channel, model, los, freq, path, sc);
            [auxGZI, snrGZI{i,j,sc}] =
GZI(Nu(i),Nr,Nt,sigma2,Pt,(i+j)+seed_rng, channel, model, los, freq, path,
sc);
            [auxGMI, snrGMI{i,j,sc}] =
GMI(Nu(i),Nr,Nt,sigma2,Pt,(i+j)+seed_rng, channel, model, los, freq, path,
sc);
            [auxZF, snrZF{i,j,sc}]   = ZF(Nr,Nu(i),Nt,Pt,sigma2,
(i+j)+seed_rng, channel, model, los, freq, path, sc);
            maxBD(i,j,sc) = max(auxBD);
            minBD(i,j,sc) = min(auxBD);
            maxGZI(i,j,sc) = max(auxGZI);
            minGZI(i,j,sc) = min(auxGZI);
            maxGMI(i,j,sc) = max(auxGMI);
            minGMI(i,j,sc) = min(auxGMI);
            maxZF(i,j,sc) = max(auxZF);
            minZF(i,j,sc) = min(auxZF);
            SR(i,j,sc) = sum(auxBD);
            SR_GZI(i,j,sc) = sum(auxGZI);
            SR_GMI(i,j,sc) = sum(auxGMI);
            SR_ZF(i,j,sc) = sum(auxZF);
        end
    end
    disp(['Progress: ' num2str(sc) '/' num2str(sb(end))]);
```

UNIVERSITAT
POLITÈCNICA
DE VALÈNCIA

_TELECOM ESCUELA
TÉCNICA VLC SUPERIOR
DE INGENIERÍA DE
TELECOMUNICACIÓN

```matlab
end

%% Calc average SNR each case
avgSNRBD  = zeros(Nu(end),Nrep,sb(end),Nu(end));
avgSNRGZI = zeros(Nu(end),Nrep,sb(end),Nu(end));
avgSNRGMI = zeros(Nu(end),Nrep,sb(end),Nu(end));
avgSNRZF  = zeros(Nu(end),Nrep,sb(end),Nu(end));

for sc = sb % Average over spatial streams & extract the data to a simpler to
navigate format
    for i = Nu
        for j = 1:Nrep
            auxBD  = mean(snrBD{i,j,sc},1)';
            auxGZI = mean(snrGZI{i,j,sc},1)';
            auxGMI = mean(snrGMI{i,j,sc},1)';
            auxZF  = mean(snrZF{i,j,sc},1)';
            for m = 1:i
            avgSNRBD(i,j,sc,m) =  auxBD(m);
            avgSNRGZI(i,j,sc,m) =  auxGZI(m);
            avgSNRGMI(i,j,sc,m) =  auxGMI(m);
            avgSNRZF(i,j,sc,m) =  auxZF(m);
            end
        end
    end
end

% Average repetitions & subcarriers
avgSNRBD  = reshape(mean(mean(avgSNRBD(:,:,sb,:),3),2),Nu(end),Nu(end));
avgSNRGZI = reshape(mean(mean(avgSNRGZI(:,:,sb,:),3),2),Nu(end),Nu(end));
avgSNRGMI = reshape(mean(mean(avgSNRGMI(:,:,sb,:),3),2),Nu(end),Nu(end));
avgSNRZF  = reshape(mean(mean(avgSNRZF(:,:,sb,:),3),2),Nu(end),Nu(end));

% Mean user SNR

avgSNRBDu  = sum(avgSNRBD,2)./Nu';
avgSNRGZIu = sum(avgSNRGZI,2)./Nu';
avgSNRGMIu = sum(avgSNRGMI,2)./Nu';
avgSNRZFu  = sum(avgSNRZF,2)./Nu';


% Mean over precoders
meanSNR = mean([avgSNRBDu avgSNRGZIu avgSNRGMIu avgSNRZFu],2);
%%

% Graph 1. Capacity vs number of users
figure
plot(Nu,mean(sum(SR,3),2), 'xb-')
hold on
plot(Nu,mean(sum(SR_GZI,3),2), 'dr-')
plot(Nu,mean(sum(SR_GMI,3),2), 'sk-')
plot(Nu,mean(sum(SR_ZF,3),2), 'mo-')

plot(Nu,mean(sum(maxBD,3),2),'xb--')
plot(Nu,mean(sum(minBD,3),2),'xb-.')

plot(Nu,mean(sum(maxGZI,3),2),'dr--')
plot(Nu,mean(sum(minGZI,3),2),'dr-.')
```

```matlab
plot(Nu,mean(sum(maxGMI,3),2),'sk--')
plot(Nu,mean(sum(minGMI,3),2),'sk-.')

plot(Nu,mean(sum(maxZF,3),2),'mo--')
plot(Nu,mean(sum(minZF,3),2),'mo-.')

grid
xlabel 'Number of users'
ylabel 'Capacity'
 title ({'Sum capacity over subcarriers'; ['SNR(dB) over number of users :
']; [num2str(meanSNR')]})
legend ('BD','GZI','GMI', 'ZF','Best user BD', 'Worst user BD', 'Best user
GZI', 'Worst user GZI', 'Best user GMI', 'Worst user GMI', 'Best user ZF',
'Worst user ZF')


%% Graph 2
figure
for Us =1:4
    subplot(2,2,Us)
plot(sb, squeeze(sum(mean(SR(Us,:,sb),2),1)),'xb-')
hold on
plot(sb, squeeze(sum(mean(SR_GZI(Us,:,sb),2),1)), 'dr-')
plot(sb, squeeze(sum(mean(SR_GMI(Us,:,sb),2),1)), 'sk-')
plot(sb, squeeze(sum(mean(SR_ZF(Us,:,sb),2),1)), 'mo-')
grid
ylabel 'Capacity [bits/(s Hz)]'
title (['Sum capacity for ' num2str(Us) ' Users'])
xlabel Subcarrier
legend ('BD', 'GZI', 'GMI', 'ZF')

end
end
disp 'End'


function [sum_rate, SNR] = ZF(Nr,Nu,Nt,Ptot,sigma2,seed,channel, model, los,
freq, path, sc)
if nargin ==0
    Nr = 2;
    Nu = 2;
    Nt = 4;
    Ptot =1;
    seed = 100;%sum(clock);
    channel = 1;
    sigma2 = 1;
end
if nargin <= 6
    channel = 1; % If not specified random channel
end
if nargin < 12 && ~channel
    model = 'B';
    los = 1;
    freq = '5';
    sc = 1;
```

```matlab
end

if channel
    randn('seed',seed);

    % % Generating the channels from the AP to the stations
    H = randn(Nr*Nu,Nt) + 1j*randn(Nr*Nu,Nt);
else
    H = ReadChannel(model,los,seed,1,freq,path);
    H = H(1:Nr*Nu, 1:Nt, sc)*sqrt(256);
end


%% Channel Invers

PZF = H'*(H*H')^-1;

% % Total power constraint

for i = 1:Nu
    PZF_norm(:,(i-1)*Nr+1:i*Nr) = PZF(:,(i-
1)*Nr+1:i*Nr).*sqrt((Ptot/Nu)/norm(PZF(:,(i-1)*Nr+1:i*Nr),'fro')^2);

    % Received power
    RxPower(:,:,i) = H((i-1)*Nr+1:i*Nr,:)*PZF_norm(:,(i-
1)*Nr+1:i*Nr).*conj(H((i-1)*Nr+1:i*Nr,:)*PZF_norm(:,(i-1)*Nr+1:i*Nr));
    % For each user, calculate sum_rate
end
for i = 1:Nu
    sum_rate(i) = 0;
    SNR(:,i) = diag(10*log10(RxPower(:,:,i)./sigma2));
    for j = 1:Nr
        sum_rate(i) = sum_rate(i) + log2(1+RxPower(j,j,i)./sigma2);
    end
end
end


function [sum_rate, SNR] = BD(Nr, Nu, Nt, Ptot, sigma2, seed, channel, model,
los, freq, path, sc)
if nargin ==0
    Nr = 2;
    Nu = 2;
    Nt = 4;
    Ptot =1;
    seed = 100;%sum(clock);
    channel = 1;
    sigma2 = 1;
end
if nargin <= 6
    channel = 1; % If not specified random channel
end
if nargin < 12 && ~channel
    model = 'B';
    los = 1;
    freq = '5';
```

```matlab
        sc = 1;
    end
%% Assuming U is available at the AP
if channel
    randn('seed',seed);
    H = randn(Nr*Nu,Nt) + 1j*randn(Nr*Nu,Nt);
else
    H = ReadChannel(model,los,seed,1,freq,path);
    H = H(1:Nr*Nu, 1:Nt, sc)*sqrt(256);
end
for i=1:Nu

    % Get the user's channel
    ss_u(i,:) = (1+(i-1)*Nr):i*Nr;  % Spatial streams assigned to each user
    H_a(:,:,i) = H(ss_u(i,:),:);
end

%% First SVD
for i = 1:Nu
    if Nu ~=1 % MU
        n = 0;
        for j = setdiff(1:Nu,i)
            H_b(n*Nr+1:(n+1)*Nr,:,i) = H_a(:,:,j);
            n = n+1;
        end
    else % SU case
        H_b(:,:,i) = H([],:);
    end
    [Ub(:,:,i) Sb(:,:,i) Vb(:,:,i)] = svd(H_b(:,:,i));
    Vb_0(:,:,i) = Vb(:, (Nu-1)*Nr + 1:end,i);
end


%% Second SVD
for i = 1:Nu
    [Uc(:,:,i) Sc(:,:,i) Vc(:,:,i)] = svd(H_a(:,:,i)*Vb_0(:,:,i));
    Vb_1(:,:,i) = Vc(:,1:Nr,i);
end

%% Calculating the precoders
for i = 1:Nu
    M(:,:,i) = Vb_0(:,:,i)*Vb_1(:,:,i);
    M(:,:,i) = M(:,:,i).*sqrt((Ptot/Nu)/(norm(M(:,:,i),'fro')^2));
end


% MU BD
for i = 1:Nu
    received_power_MU_BD_with_U_at_AP(1:Nr,1:Nr,i) =
(Uc(:,:,i)'*H_a(:,:,i)*M(:,:,i)).*conj((Uc(:,:,i)'*H_a(:,:,i)*M(:,:,i)));
    sum_rate_MU(i) = 0;
    SNR(:,i) =
diag(10*log10(received_power_MU_BD_with_U_at_AP(:,:,i)./sigma2));
    for j = 1:Nr
        sum_rate_MU(i) = sum_rate_MU(i) +
log2(1+received_power_MU_BD_with_U_at_AP(j,j,i)./sigma2);
    end
```

UNIVERSITAT
POLITÈCNICA
DE VALÈNCIA

_ TELECOM ESCUELA
TÉCNICA VLC SUPERIOR
DE INGENIERÍA DE
TELECOMUNICACIÓN

```matlab
    end
sum_rate = sum_rate_MU;
end

function [Sum_Rate, SNR] = GZI(Nu,Nr,Nt,sigma2,Ptot,seed,channel, model, los,
freq, path, sc)
if nargin ==0
    Nr = 2;
    Nu = 2;
    Nt = 4;
    Ptot =1;
    seed = 100;%sum(clock);
    channel = 1;
    sigma2 = 1;
end
if nargin <= 6
    channel = 1; % If not specified random channel
end
if nargin < 12 && ~channel
    model = 'B';
    los = 1;
    freq = '5';
    sc = 1;
end

if channel
    randn('seed',seed);
    H = randn(Nr*Nu,Nt) + 1j*randn(Nr*Nu,Nt);
else
    H = ReadChannel(model,los,seed,1,freq,path);
    H = H(1:Nr*Nu, 1:Nt, sc)*sqrt(256);
end
for i=1:Nu
    % Get the user's channel
    ss_u(i,:) = (1+(i-1)*Nr):i*Nr;  % Spatial streams assigned to each user
end

HH = H'*(H*H')^-1;
for i = 1:Nu
    % Get user channel
    Hu(:,:,i) = H(ss_u(i,:),:);
    % Pseudo invers of the channe;
    H_inv(:,:,i) = HH(:,ss_u(i,:));%Hu(:,:,i)'*(Hu(:,:,i)*Hu(:,:,i)')^-1;
    % QR decomposition of the invers
    [Q(:,:,i), ~] =qr(H_inv(:,:,i),0);


    % Second SVD
    [U(:,:,i),S(:,:,i),V(:,:,i)] = svd(Hu(:,:,i)*Q(:,:,i));
    P(:,:,i) = Q(:,:,i)*V(:,:,i);
    P(:,:,i) = P(:,:,i)*sqrt((Ptot/Nu)/norm(P(:,:,i),'fro')^2);

    M(:,:,i) = U(:,:,i)';

end
```

```matlab
%% Calculate sum-rate

for i = 1:Nu
    rx_power(:,:,i) =
(M(:,:,i)*Hu(:,:,i)*P(:,:,i)).*conj((M(:,:,i)*Hu(:,:,i)*P(:,:,i)));
    Sum_Rate(i) = 0;
    SNR(:,i) = diag(10*log10(rx_power(:,:,i)./sigma2));

    for j= 1:Nr
        Sum_Rate(i) = Sum_Rate(i) + log2(1+rx_power(j,j,i)./sigma2);
    end

end
end

function [Sum_Rate, SNR] = GMI(Nu,Nr,Nt,sigma2,Ptot,seed,channel, model, los,
freq, path, sc)
if nargin ==0
    Nr = 2;
    Nu = 2;
    Nt = 4;
    Ptot =1;
    seed = 100;%sum(clock);
    channel = 1;
    sigma2 = 1;
end
if nargin <= 6
    channel = 1; % If not specified random channel
end
if nargin < 12 && ~channel
    model = 'B';
    los = 1;
    freq = '5';
    sc = 1;
end

if channel
    randn('seed',seed);
    H = randn(Nr*Nu,Nt) + 1j*randn(Nr*Nu,Nt);
else
    H = ReadChannel(model,los,seed,1,freq,path);
    H = H(1:Nr*Nu, 1:Nt, sc)*sqrt(256);
end

for i=1:Nu
    % Get the user's channel
    ss_u(i,:) = (1+(i-1)*Nr):i*Nr;  % Spatial streams assigned to each user
end

% Get parameter alfa
alfa = Nr*Nu*sigma2/Ptot;
for i = 1:Nu
    % Get user channel
    Hu(:,:,i) = H(ss_u(i,:),:);
    % Pseudo invers of the channe;
    H_mmse_T = (H'*H+alfa*eye(Nt))^-1*H';
    H_mmse(:,:,i) = H_mmse_T(:,ss_u(i,:));
```

```matlab
    % QR decomposition of the invers
    [Q(:,:,i), ~] =qr(H_mmse(:,:,i),0);
    %
    % Transmit matrix
    % Sumatory
    aux = zeros(Nt,Nr);
    for j = 1:Nu
        Hk = H(ss_u(j,:),:);
        aux = aux + Hk'*Hk*Q(:,:,i);
    end
    % Get the unitary matrix
    Tu(:,:,i) = (Q(:,:,i)'*aux+alfa*eye(Nr))^-
1*Q(:,:,i)'*Hu(:,:,i)'*Hu(:,:,i)*Q(:,:,i);
end
% Scale facotr Beta
aux = 0;
for i = 1:Nu
    aux = aux+trace(Tu(:,:,i)'*Tu(:,:,i));
end

beta = sqrt(Ptot)*(aux)^-1/2;
% Final transmit matrix
T = beta*Tu;
%T = Tu;
for i = 1:Nu
    % Second SVD
    [U(:,:,i),S(:,:,i),V(:,:,i)] = svd(Hu(:,:,i)*Q(:,:,i)*T(:,:,i));
    P(:,:,i) = Q(:,:,i)*T(:,:,i)*V(:,:,i);
    S(:,:,i) = S(:,:,i)*sqrt((Ptot/Nu)/norm(P(:,:,i),'fro')^2);
    P(:,:,i) = P(:,:,i)*sqrt((Ptot/Nu)/norm(P(:,:,i),'fro')^2);
    M(:,:,i) = U(:,:,i)';

end


%% Calculate sum-rate

for i = 1:Nu
    rx_power(:,:,i) =
(M(:,:,i)*Hu(:,:,i)*P(:,:,i)).*conj((M(:,:,i)*Hu(:,:,i)*P(:,:,i)));
end


for j = 1:Nu
    for i = 1:Nr
        aux = 0;
        for n = 1:Nu
            if n~=j
                aux = aux + norm(M(i,:,j)*(H(ss_u(j,i),:)*P(:,i,n)))^2;
            end
        end
        SNR(j,i) = S(i,i,j).^2/(sigma2 + aux);
    end
end

Sum_Rate = sum(log2(1+SNR),2);
```

```
SNR = (10*log10(SNR'));
end
```